ANALYTICAL AND EXPERIMENTAL STUDIES OF DRAG EMBEDMENT ANCHORS AND SUCTION CAISSONS

A Thesis

by

RYAN DEKE BEEMER

Submitted to the Office of Graduate Studies of
Texas A&M University
in partial fulfillment of the requirements for the degree of

MASTER OF SCIENCE

May 2011

Major Subject: Civil Engineering

Analytical and Experimental Studies of Drag Embedment Anchors and Suction Caissons

ANALYTICAL AND EXPERIMENTAL STUDIES OF DRAG EMBEDMENT ANCHORS AND SUCTION CAISSONS

A Thesis

by

RYAN DEKE BEEMER

Submitted to the Office of Graduate Studies of
Texas A&M University
in partial fulfillment of the requirements for the degree of

MASTER OF SCIENCE

Approved by:

Chair of Committee,	Charles Aubeny
Committee Members,	Giovanna Biscontin
	Jerome Schubert
Head of Department,	John Niedzwecki

May 2011

Major Subject: Civil Engineering

ABSTRACT

Analytical and Experimental Studies of Drag Embedment Anchors and Suction Caissons. (May 2011)
Ryan Deke Beemer, B.S., Washington State University
Chair of Advisory Committee: Dr. Charles Aubeny

The need for experimental and analytical modeling in the field of deep water offshore anchoring technologies is high. Suction caisson and drag embedment anchors (DEA) are common anchors used for mooring structures in deep water. The installation process of drag embedment anchors has been highly empirical, employing a trial and error methodology. In the past decade analytical methods have been derived for modeling DEA installation trajectories. However, obtaining calibration data for these models has not been economical. The development of a small scale experimental apparatus, known as the Laponite Tank, was developed for this thesis. The Laponite Tank provides a quick and economical means of measuring DEA trajectories, visually. The experimental data can then be used for calibrating models. The installation process of suctions caissons has benefited from from a more rational approach. Nevertheless, these methods require refinement and removal methodology requires development. In this thesis, an algorithm for modeling suction caisson installation in clay has been presented. An analytical method and modeling algorithm for removal processes of suction caissons in clay was also developed. The installation and removal models were calibrated to field data. These analytical and experimental studies can provide a better understanding of installation of drag embedment anchors and the installation and removal of suction caissons.

ACKNOWLEDGEMENTS

I would like to foremost thank my committee chair and adviser, Dr. Aubeny. Thank you for your time and assistance over the course of my academic endeavors. I would also like to thank my committee members, Dr. Biscontin and Dr. Schubert, for their help and input. Thank you.

I would like to thank Delmar Systems Inc. and Evan Zimmerman for the testing equipment and field data. Connections between industry and academia, such as these, are invaluable. Thank you.

I would also like to thank my family, especially my parents for their moral support and financial aid. Thank you, I could not have completed this with out you. And appreciation goes to my siblings and grandparents for their interest in my research, feigned or real. I feel loved having family willing to listen to me talk about my research. Thank you.

Finally, I would like to thank my friends. To my friends in College Station, your help in preserving my sanity is greatly appreciated. Thank you. And to my friends from California, having a connection to back home is very meaningful to me. Thank you.

NOMENCLATURE

θ_0	anchor line angle at the mudline
C	anchor line diameter of 1.58 mm (1/16 in)
DEA	drag embedment anchor
dz	incremental step size for computer programs
ft	feet
fps	frames per second
GUI	graphic user interface
in	inch
k	soil strength gradient
MODUS	mobile offshore drilling units
N_c	dimensionless bearing factor
N_c	dimensionless bearing factor input for caisson programs
N_{ca}	anchor line bearing factor
N_e	anchor bearing factor
N_q	dimensionless bearing factor input for caisson programs
S_{u0}	soil shear strength at mudline
tiff	tagged image file format
TLPS	tension leg platforms
V	anchor line diameter of 3.18 mm (1/8 in)
W	anchor line diameter of 0.96 mm

TABLE OF CONTENTS

Page

Page

LIST OF TABLES

LIST OF FIGURES

FIGURE Page

FIGURE Page

FIGURE Page

1 INTRODUCTION

1.1 Overview

Off shore foundation technologies have been in a continuously evolved since their inception. Much of this evolution has been driven by the need to install structures in deeper and deeper water (Aubeny et al., 2001). Traditionally structures in relatively shallow water have consisted of large vertical towers supporting the platform's gravity load. The move to deep water has made these structures impractical from the stand point of both construction and their ability to resisting ocean and wind loading. Consequently floating structures moored to the sea bottom are often the system of choice for offshore hydrocarbon exploration and production. Such structures include mobile offshore drilling units (MODUS) for explorations, tension leg platforms (TLPS) and spars for production facilities.

Foundation systems for floating structures differ significantly from fixed systems in shallow water. Shallow water foundations must resist compressive loads from the structures self weight, similar to onshore foundations. By contrast their deep water counterparts must resist tension loads from buoyant forces, similar to an anchored hot air balloon. Suction caissons and drag embedment anchors (DEAs), Fig. 1.1,are two systems commonly used for mooring floating structures. These technologies are currently being used in the offshore industry and are proving successful. However, for these technologies to be used with greater confidence their predictability and reliability must be improved.

The goal of this thesis is to increase the reliability of suction caissons and DEAs , this has been done by creating and calibrating analytical and experimental models of these anchors. In practice the installation of drag embedment DEAs is highly empirical. A trial and error method is used for placement of the anchors, which can lead to multiple

---

This thesis follows the style of the *Journal of Geotechnical and Geoenviromental Engineering.*

installation attempts and uncertainty in anchor embedment depth and load capacity. Scale modeling of DEA was conducted a transparent synthetic soil, Laponite® RD. An image processing program was then developed to analyze and convert the visual trajectories into Cartesian coordinates. These trajectories have thus been used to quantify an analytic model developed from Aubeny et al. (2008). The analysis of suction caisson installation is based on a more rational approach than that currently for DEAs. Nevertheless the existing methods of analysis require refinement and calibration. An analytical model of suction caisson installation and extraction was developed in this research is largely based in the methods described by Anderson et al. (2005). Proprietary data from the offshore anchoring technologies company Delmar Systems Inc. will be used to calibrate the suction caisson models.

Fig. 1.1: Suction caisson (left) and DEA (right) (Courtesy of Delmar)

1.2 Suction Caissons

The first stage of this research involved the development of a method for predicting the

required under and over pressures during the installation and removal processes respectively. During the installation process the internal pressure within the suction caisson is reduced. This applied under pressure results in the suction caisson being embedded into the seabed; therefore, the under-pressure must be sufficiently great to over come the soil resistance to penetration. However, there does exist a critical under pressure in which a plug heave failure will result: that is, the suction a inside the caisson chamber exceeds the soil resistance forces holding the plug in place. Therefore, suction caisson installation involves a delicate balance in between sufficient application of under-pressure to advance the caisson and inducing a plug heave failure. If installation cannot be achieved without an adequate margin of safety against a plug heave failure, a larger and therefore more expensive caisson must be used. In addition to a catastrophic failure of the soil plug, a more modest plug heave occurs during caisson installation. This is a simple consequence of a portion of the soil volume being displaced by the caisson into the caisson. This type of plug heave is not catastrophic, but it will result in a modest reduction in the maximum penetration depth. This reduction in the caisson penetration depth will reduce the operational load capacity of the caisson and must therefore be reliably predicted in advance. This thesis has developed an analytical method and computer algorithm for establishing required and critical under pressures with respect to installation depth. The analytical method was adapted from the work of Anderson et al. (2005). While the computer program was developed to utilize the said analytical method. These should result in economical and safe suction caisson installation.

Similarly an analytical method and computer algorithm was also developed to predicted required and critical over pressures with respect to caisson depth during the removal process. For temporary anchor applications, suction caisson must be removed by the application of positive internal pressure, which is supplemented by a winch load. During suction caisson installation, the self-weight of the caisson assists penetration. However, during caisson extraction, the over pressure must overcome the caisson's self-weight in addition to the soil resistance forces; therefore, required over-pressure tends to be much

large than required under-pressure. Though, since the over pressure now acts downward, a potential plug heave failure is no longer an issue. However, in the latter stages of extraction excessive over-pressure can cause a blowout. That is, a soil failure exactly analogous to a classical shallow bearing capacity failure. The failure of the soil around the caisson can result in decreased strength and can disturb nearby anchors and or structures. In developing an analytical method to predict required and critical over-pressures with suction caisson depth, a means has been provided to more quickly and safely remove suction caissons. This thesis outlines the development of the suction caisson removal analytical method. Anderson et al. (2005) did not outline the removal process so it was necessary for it to be developed. A computer algorithm was also developed for the analytical method's application.

Both the models where then calibrated to data collected by Delmar. Delmar provided installation and removal data collected from projects conducted in the Gulf of Mexico. The data includes 20 installation records and six removal records. Two sites encompass the testing area: 17 installation records and three removal records form one site, with the remaining records coming from another site. Soil strength data from the two sites will also be provided: five from the first site and four from the second.

1.3 Drag Embedment Anchors

DEAs are currently favored in the field because of their high capacity to weight ratios and easy installation process. However, they tend to have large uncertainty in their placement and therefore capacity. Unlike many of their counterparts DEAs are installed tens of meters below the mudline making their exact installation trajectory and final location difficult to ascertain. Very few installations have been in the field were exact trajectory was recorded; this is mainly due to the cost required in obtaining the data. Therefore there is a minimal amount of data available to for verifying and proving analytical models. This can be seen in the use of only three experimental tests to correlate models in Aubeny et al. (2008). There is a need for an easy way to obtain DEA trajectories at low cost.

In Aubeny et al. (2008) a translation and rotational modeling system was used to analytically model the trajectory of a DEAs. The model was proved successful by comparison to the three field tests mentioned above. This model was further optimized in Aubeny and Chi (2010a) resulting in the removal of the translation portion of the model. The field tests data available from Aubeny et al.(2008) was only conducted with Bruce MK2 anchors, one of many currently available on the market. Testing simplified anchors with traits that mimic those available would be invaluable in in understanding anchor behavior. However, the amount of testing necessary to verify these anchors is extensive and the cost of true or even large scale field experiments would be significant. Therefore, a small scale testing apparatus (Laponite Tank) and methodology was developed making qualitative of verification the analytical model to new anchor types economically feasible.

A small scale testing apparatus was developed to provide visual and measurable installation trajectories for DEA model verification and prototype anchor testing. The offshore anchoring company Delmar provided Texas A&M University with multiple scale model anchors and a reinforced glass tank for testing. The tank is 1.82 m (6 ft) long by 61 cm (2 ft) wide by 1.2 m (4 ft) deep. Laponite RD, a product from Southern Clay Products was used as a synthetic translucent soil. The experiments were recorded on video and a computer program using visual image analysis techniques was developed to quantify the anchor's trajectory through the Laponite.

Laponite is a synthetic layered silicate, when combined with tap water at concentration greater than two percent by mass Laponite, a gel is formed. Laponite is similar to natural clays in chemical structure, however it differs in three significant ways. One, any Laponite gel that can be formulated will have undrained shear strength significantly lower than soil. Two, Laponite gel exhibits shear thinning properties while natural clays are shear thickening. Three, Laponite is translucent while natural clays are opaque. The translucency of Laponite allows the total trajectory of the anchor to be visually tracked and recorded in real time as it is installed, natural clays do not allow this. Thus, the selected testing median has a low strength in order to have translucent properties. To

accommodate this, testing of the analytical model must been at low shear strength, in order to obtain quantitative correlations. However, qualitative correlations can still occur with site specific undrained shear strengths. The discrepancy in shearing properties can be minimized with anchor embedment rates. Soil strength tests are preformed at low rates to minimize shear thickening effects, so the embedment tests will be performed at low rates to minimize shear thinning effects.

A video camera was used to record the real time results of the experiments. The footage was then digitized and broken into individual frames. The typical frame rate of a video camera is 29 frames per second (fps). Digital grayscale images are simply matrices consisting of values between zero and one to symbolize levels black and white respectively. MATLAB is a programming language design to operate matrices efficiently, making it a good choice for image manipulation. MATLAB also has a number of built functions customized for visual image analysis. MATLAB was used to create a program to read in the individual frames of the experimental footage, isolate the image of the anchor from the background, and track its Cartesian coordinates as it move through the images.

With this program different anchor properties were tested in the tank and compared to result obtain from the above analytical method. For example for this thesis the effect of anchor line diameter on embedment depth was on of the properties examined. The Laponite Tank was able to verify that an increase in anchor line diameter will result in a qualitative decrease in DEA embedment.

2 BACKGROUND

2.1 Overview

A review of background information is provided in the following subsection. Included is information on two offshore anchoring technologies, drag embedment anchors and suction caissons. This includes a review of the state-of-practice study by Anderson et al. (2005) on suction caissons installation and a literature review of analytical modeling techniques of DEA trajectories. A final subsection has been provided on general knowledge regarding digital image processing.

2.2 Anchoring Technologies

2.2.1 Suction Caissons

Suction caissons are popularly used for the anchoring of temporary offshore structures. Suctions caissons are reusable, capable of accurate installation, and amenable to reliable predictions in load capacity. However, their cost to capacity ratio is relatively high. When used multiple times suction caissons become cost effective.

Suction caissons are cylindrical tubes of various lengths and diameters. There tops are capped. An example image is provided in Fig. 2.1. During installation the caisson's self-weight partially embeds it into the soil. A system of hoses then allows pumping from the internal camber resulting in a decrease of the internal water pressure. This negative differential pressure termed 'suction' advances the caisson into the seabed. Conversely, for caisson removal, the internal pressure can be increased, thereby extracting the caisson from the seabed.

Large suctions caissons require internal stiffeners to keep their shape during storage and transportation. These stiffeners can become quite complicated and can impact installation and removal processes, an example cross-section be seen in Fig. 2.2. Typical configurations can include rings along the interior wall and plates across the cavity. Stiffeners are designed for structural purposes. Geotechnical considerations are

secondary, although the soil resistance generate by the stiffeners must be considered in the installation analysis.

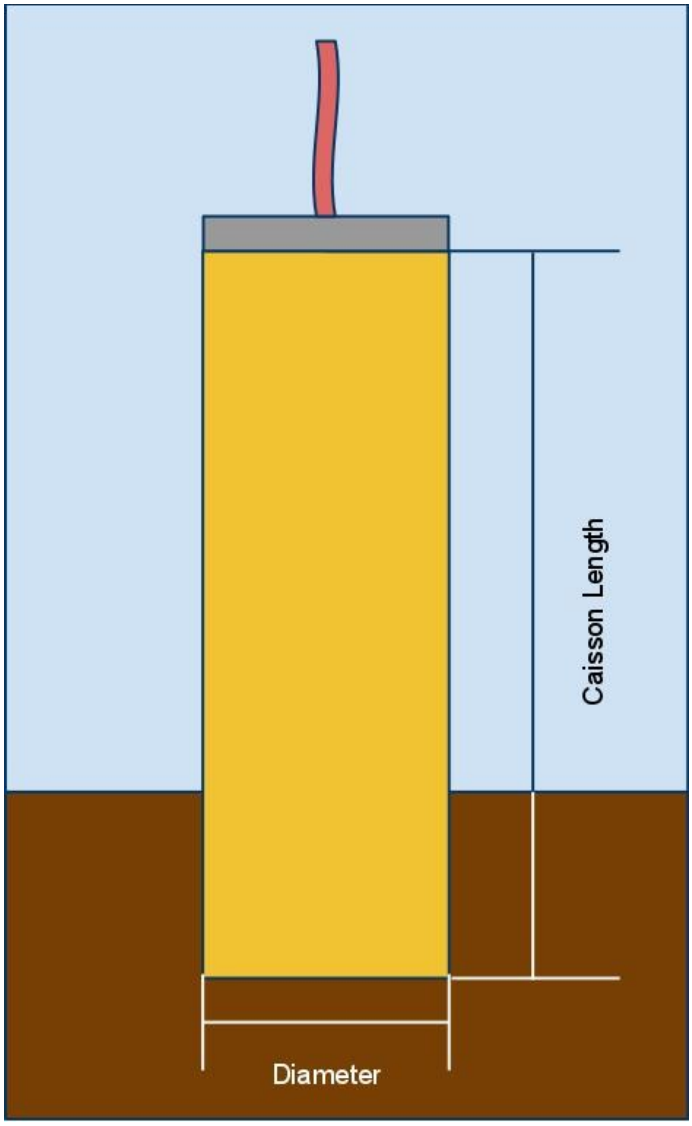

Fig. 2.1: Example suction caisson

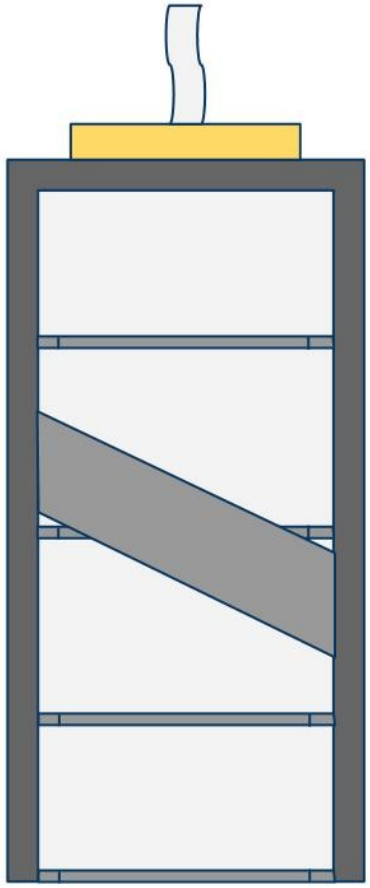

Fig. 2.2: Example of internal stiffeners within large suction caissons

2.2.2 Drag Embedment Anchors

Drag embedment anchors are preferred for use in anchoring because of their low cost-to-capacity ratio. Their high capacity comes from their ability to embed tens of meters into the seabed were soil shear strength is much higher. However, with the anchor at these depths it becomes difficult to reliably predict it's location. This introduces uncertainty in predicting capacity. Though extremely efficient, DEAs entail higher uncertainty than other types of anchors.

Drag embedment anchors typical consist of two parts: a shank and a fluke. Geometric parameters of concern are fluke length, fluke area, shank length, and fluke-shank angle, Fig. 2.3. DEAs are installed with an applied anchor line force. This results in the anchor diving into the seabed, as seen in Fig. 2.4. During embedment the anchor line is typical sufficiently long to allow the anchor line angle at the mudline to be zero.

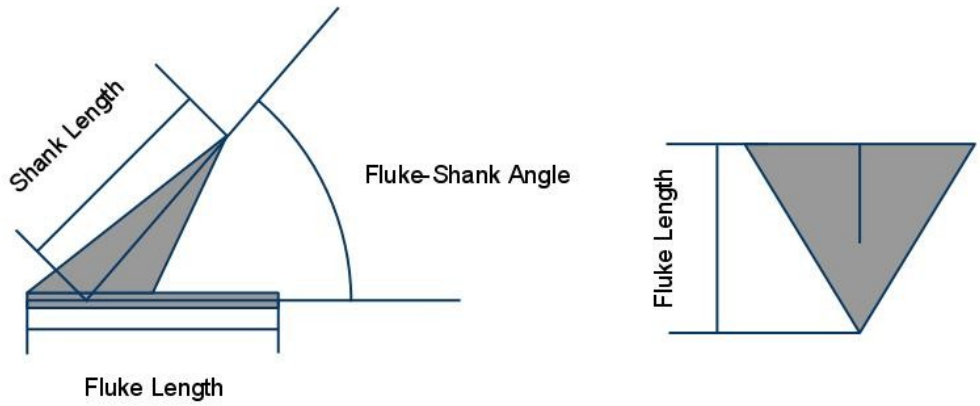

Fig. 2.3: Example drag embedment anchor

2.3 Literature Review

2.3.1 Suction Caissons

Research on suction caissons has been conducted at Texas A&M University since at least 2000. This research has been limited to the capacity of suction caissons. Research on this subject was investigated in Moon (2000), Han (2002) and Sharma (2004). Research for this thesis was on caisson installation and removal.

For suction caisson installation *Suction Anchors for Deepwater Application* by K. H.

Anderson et al. (2005) is a useful source. Extensive recommendations are provided for evaluating soil resistant forces during installation. Included also are criterion for effects such as plug heave, critical under-pressure, and factor of safety. Anderson et al. (2005) also examined suction caisson capacity. Furthermore proprietary data from industry was collected and displayed in the paper. The theory in this paper is cover is Subsection 3.1 in the development of an algorithm for modeling suction caisson installation.

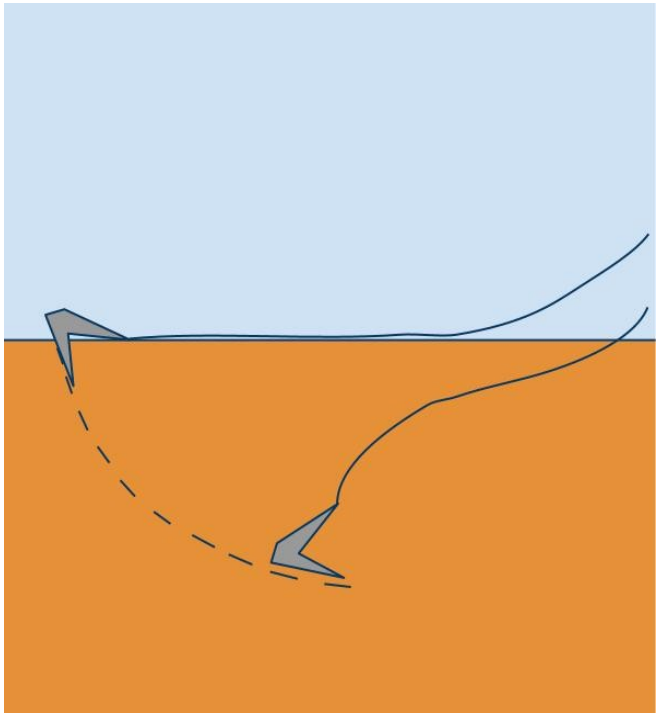

Fig. 2.4: Example DEA trajectory

2.3.2 Drag Embedment Anchors

Research on drag embedment anchors has been conducted at Texas A&M university since 2002. Yoon (2002) and Kim (2005) examined DEA capacity. Veniamin (2006) focused of DEA anchor lines. Yang (2008) and Chi (2010) examined out-of-plane

loading of DEAs. Chi (2010) also investigated in-plane DEA trajectories. In this thesis research was on small scale experimental modeling of DEA trajectories.

In Section 5 anchor trajectory is modeled using analytical methods. These equations have come about through much research. *Predictions of Anchor Trajectory During Drag Embedment in Soft Clay*, Aubeny et al. (2008) provided a means of calculating DEA trajectory from rate of change in the anchor line angle at the shackle with respect to the vertical direction. This was described in a translational phase and a rotational phase. It also provided an algorithm for calculating anchor trajectory from this rate in change of the anchor line angle. The paper also provided means of determining anchor capacity.

Further research indicated that the translation phase was unnecessary. This was illustrated in *Mechanics of Drag Embedment Anchors in a Soft Seabed,* Aubeny and Chi (2010). In this paper the transitional phase was removed and DEA became dependent of anchor rotation. This paper also included means for including a rate of change of the anchor line angle at the mudline. Anchor capacity was also discussed. Finally the paper provided an updated algorithm for calculating anchor trajectory.

Research in this thesis utilized methodology outline in *Soil Impact on Non-Stationary Anchor Performance,* Aubeny et al. (2009). This is a simplified form of the work presented in Aubeny and Chi (2010). Anchor trajectory is determined from the rate in change of the anchor line angle at the shackle point and this is only dependent on anchor rotation. However, Aubeny et al. (2009) assumes a constant anchor line angle at the mudline. This simplifies the process of calculating anchor trajectory. This paper also discusses trajectories of vertically loaded anchors and dealing with anchor with complex geometry. The theory of Aubeny et al. (2009) is covered further in Subsection 5.2.

2.4 Image Processing

The following is a general description of digital image processing, assuming 8 bit images. As image processing is not typical area associated with geotechnical engineering this subsection has been included. Digital image processing conducted in subsection 4.2 was completed utilizing MATLAB. More detailed and further information on digital

image processing in MATLAB can be found in Alasdair McAndrew's *Introduction to Digital Image Processing with MATLAB* (McAndrew, 2004) and the MATLAB user manual.

2.4.1 Binary and Grayscale Images

The simplest image is a binary image. A binary image is mathematical represented as a matrix with entry values of either one or zero. Each entry in the matrix corresponds to a single pixel. A value of one corresponds to the color white and a value of zero corresponds to the color black. An example binary image with its corresponding matrix is shown in Fig. 2.5.

A grayscale image is slightly more complex than a binary image. As with a binary image a grayscale image is represented mathematically with a matrix. However, there are an additional 254 fractional entry values between zero and one. In this case the closer the fraction is to zero the darker the gray color and the closer the fraction is to one the lighter the gray color. It is possible to represent a grayscale image with entry values of integers from zero and 255, unless indicated this convention is assumed in this Subsection.

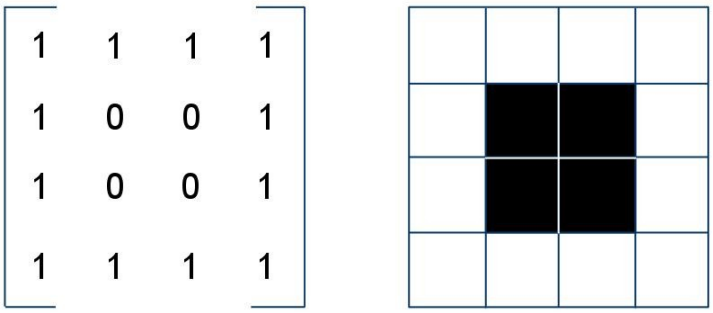

Fig. 2.5: Example binary image with matrix representation

The process of converting a grayscale image to a binary image is called thresholding. When thresholding an image a grayscale value is specified. All values greater than this number are converted to 255, becoming white. All values less than this value are converted to zero, becoming black, Fig. 2.6. By selecting different grayscale values in the thresholding process it is possible to create multiple binary images from a single grayscale image.

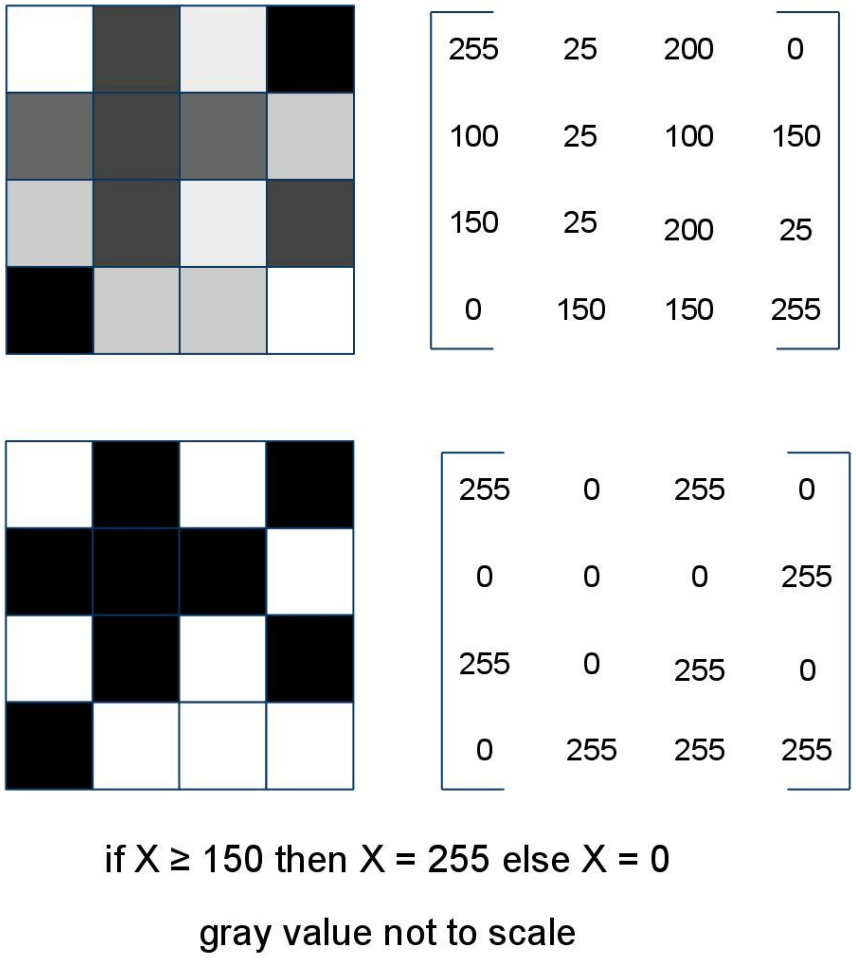

Fig. 2.6: Example of image thresholding

2.4.2 Image Mathematics

As images are mathematically matrices it is possible to preform mathematical operations with them. It is possible to add, subtract, and multiple images, amongst other operations. However, due to the nature of images there are limitations to these manipulations.

The maximum value of a matrix entry in an image is 255 and the minimum value is zero. When conducting mathematical operations with image matrices it is necessary to prevent the entry values from going beyond this range. Entry values must also be limited to integers. MATLAB has built in function that help meet these criterion. For example when adding image matrices in MATLAB it is recommended the function *imadd* is used.

2.4.2 Image Filtering

A special set of matrix operations which are useful to image processing are known as filters. By applying filters, such as averaging and median, images can be altered in specific ways. A image is filtered by passing a mask over every pixel in the image. The mask preforms a specific mathematical operation altering the pixel it is over.

The minimum size for a mask is typically three by three pixels, see Fig. 2.7. Smaller masks are possible, but require different operating parameters. Masks perform a specific mathematical operation on the pixel they are centered over based on the pixel values in the mask. In general, if a mask is extends beyond the image values are assumed to be zero. Two common filters are averaging and median.

The mask in an averaging filter will find the average of all pixels with in the mask and place that value in the center pixel. This results in a softening or blurring of the image. Fine details and contrast will be lost. The larger the mask the more blurred the image will appear. Averaging filters will also place a dark ring around the image since values beyond the image are assumed to be zero.

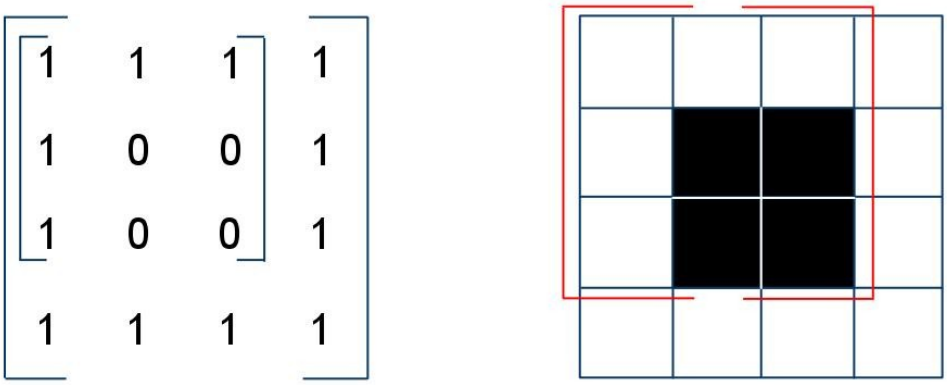

Fig. 2.7: Example of filter mask

The mask in a median filter is similar to that of an averaging filter. It calculates the average of all the pixel values within the mask however, it excludes the center pixel. This average value is then applied to the center pixel. This filter is extremely useful in removing loud noise from the image, especially salt and pepper noise. An averaging filter averages the value of a loud pixel into its neighbor while a median filter will simply replace the loud pixel with the average value of its neighbors.

3 ANALYTICAL MODELING OF SUCTION CAISSONS

3.1 Installation Model

The analytical method presented in this subsection was developed based on the detailed discussion of suction caisson installation modeling found in Anderson et al. (2005). The following paragraphs describe the analytical method specially used to create a computer program capable of predicting required under-pressure for caisson penetration and critical under-pressures at which a soil plug failure can occur.

Required under-pressure for the suction caisson was computed using a force equilibrium method. The required under-pressure for caisson penetration considers the various soil resistant forces acting on the caisson and the submerged self weight of the. These resistant forces are outer skin friction, inner skin friction, stiffener plate skin friction, stiffener bearing resistance, and tip resistance.

Skin friction is a resultant of soil adhesion to the metal shell of the suction caisson. Skin friction can be described by the following:

$$Q_s = \alpha s_u A_s \tag{3.1}$$

where: Q_s = skin friction force

α = adhesion factor = 1/S

s_u = undrained shear strength

A_s = skin surface area

S = soil sensitivity

That is, skin friction is the product of the undrained shear strength, the surface area exposed to the soil, and an adhesion factor. The adhesion factor is a scaling factor to accommodate for factors such as smearing, friction, and consolidation. Adhesion can be

approximated by the inverse of the soil sensitivity, typical two to three for installation. Outer skin friction specifically refers to the resultant force between the outside of caisson's shell and the soil in the surrounding seabed. Inner skin friction specifically refers to the resultant force between the inside wall of the suction caisson and the soil plug. Due to soil heave the height of the soil plug can be greater than the embedment depth of the caisson. Stiffener plate skin friction refers specifically to the resultant force between the structural plate stiffeners and the soil plug.

Tip resistance is the resultant force from the any surface area of the bearing normal to the soil as the suction caisson is embedded. Bearing resistance can be described by the following:

$$Q_b = \left(N_c s_u + \gamma z N_q\right) A_b \qquad (3.2)$$

where: Q_b = bearing force

N_c = dimensionless bearing factor

A_b = bearing surface area

γ = unit weight of soil

z = embedment depth

N_q = dimensionless bearing factor

The quantity N_c is an empirical bearing factor. The described area is any continuous surface which is normal to the direction of penetration of the caisson into the seabed. The two components typical impacted are the tip of the caisson and the structural stiffeners.

As undrained shear strength is dependent on depth, it is then possible to assume a depth of embedment and determine all possible resistant force on the suction caisson. This force is then equal to the required force to embed the caisson into the seabed. This can be

described by the following:

$$Q_{total} = \sum_{i=1}^{n} Q_{b_i} + \sum_{j=1}^{m} Q_{s_j} \tag{3.3}$$

where: Q_{tot} = total resistant force

n = number of bearing forces

m = number of skin friction forces

The required force then can be determined by subtracting the caissons buoyant weight from total resistant force. The required under-pressure is the required force divided by the area of the soil plug. This can be described by the following:

$$P_{in} = \frac{Q_{in}}{A_{plug}} \tag{3.4}$$

where: P_{in} = required under-pressure

Q_{in} = required embedment force = $Q_{tot} - W_s$

A_{plug} = surface area of soil plug

W_s = buoyant weight of suction caisson

The critical under pressure is then determined from equilibrium of the forces required to keep the soil plug from losing continuity from the seabed. Soil forces resisting a plug failure can be broken into internal skin friction, stiffener skin friction, and soil plug inverse bearing capacity. The inverse bearing capacity only takes into account the cohesive properties of the bearing surface, overburden forces are neglected. This can be described as follows:

$$Q_{ib} = N_c \, s_u \, A_{plug} \tag{3.5}$$

where: Q_{ib} = inverse bearing capacity of the soil plug

Thus the total resistant force against soil plug failure becomes the summation of the inverse bearing capacity, internal skin friction, and plate stiffener friction. This can be described in the following:

$$Q_{total} = Q_{ib} + \sum_{i=1}^{m} Q_{s_i} \tag{3.6}$$

The critical under-pressure becomes the total resistance force divided by the area of the soil plug, similar Eq. (3.4). Therefore by using the fact that undrained shear strength is dependent on soil depth critical under-pressure can be calculated versus embedment depth.

To determine required and critical under-pressures it is necessary to know the embedment depth and the soil plug height. As previously mentioned the soil plug height is typical greater than embedment depth. This is due to the plug heave effect. As described in Anderson et al. (2005), during embedment by under-pressure 50 percent to 100 percent of the soil volume displaced by the bearing tip of the caisson will be displaced into the suction caisson instead of the surrounding soil. For self weight installation the plug heave factor is an estimated 50 percent. This displaced soil accounts for the difference in soil plug height versus embedment depth. This difference can be calculated by the following:

$$\Delta z = \frac{\left(R_p A_{tip} z\right)}{A_{plug}} \tag{3.7}$$

where: Δz = differential height

R_p = plug heave factor

The soil plug height becomes the sum of the differential height and the embedment depth of the caisson. This can be described by the following.

$$z_{in} = z + \Delta z \tag{3.8}$$

where: z_{in} = soil plug height

With the above model, both required under-pressures can be calculated for the installation of a suction caisson into the seabed. With this data the installation process can be simulated thus increasing installation speed and reducing soil plug failures.

3.2 Removal Model

An analytical method for modeling suction caisson removals was also developed for Delmar. For suction caisson removal it was necessary to determine the required and critical over-pressures need to remove the caisson from the seabed. Though Anderson et al. (2005) provided solutions for suction caisson installation, it lacked ones for their removal. Thus one need to be created for this project. Development was started by analyzing the techniques associated with suction caisson installation outlined in Anderson et al. (2005).

It was noted that inner, outer, and stiffener skin friction would impact the resistant forces and therefore the required over-pressure. However, the caisson tip and stiffeners are no

longer applying a downward normal force against seabed, instead they are applying a upward force. This force can be calculated as an inverse bearing capacity, with the overburden force working against capacity. This can be described by the following:

$$Q_{ib} = \left(N_c s_u - \gamma z N_q \right) A_b \tag{3.9}$$

The resistant force then can be calculated as the summation of the inner skin friction, outer skin friction, stiffener skin friction, the inverse bearing capacity of the caisson tip, and the inverse bearing capacity of the stiffeners. This can be described by the following:

$$Q_{total} = \sum_{i=1}^{l} Q_{ib_i} + \sum_{j=1}^{m} Q_{s_j} \tag{3.10}$$

where: l = number of inverse bearing forces

Then due to force equilibrium, the required force to remove the caisson thus becomes the total resistant force minus the wench load plus the buoyant weight of the suction caisson. The total required over-pressure thus becomes the total required force divided by the area of the soil plug. This can be described as the following:

$$P_{out} = \frac{Q_{out}}{A_{plug}} \tag{3.11}$$

where: P_{out} = required over-pressure

Q_{out} = required removal force = $Q_{tot} - W_w + W_s$

W_w = applied wench load

Then by making undrained shear strength a function of depth it is possible to get required over-pressure as a function of depth over the suction caissons removal process.

Critical over-pressure is also determined by force equilibrium. A failure due to excess over-pressure results in the soil in the seabed failing allowing the soil plug to be blown out of the caisson. At shallow depths a plug blowout is unlikely. However, in the latter stages of caisson extraction, the proximity to a free surface can lead to a blowout. If the caisson cannot be extracted without a reasonable factor of safety during this stage of extraction, a winch load can be applied to reduce the overpressure requirement. Plug blowout can be prevented by ensuring that the over-pressure does not exceed the forces holding the soil plug in the caisson and the bearing capacity of the soil plug. The resistant forces then are inner skin friction, stiffener skin friction, stiffener inverse bearing capacity, and the bearing capacity of the soil plug.

Thus with the total resistant force and by force equilibrium the total critical force is the summation of the above mentioned forces. This can be described by an equation similar to Eq. (3.10). Then the critical over-pressure can then be determined by dividing the critical force by the surface area of the soil plug, similar to the equation shown in Eq. (3.11).

Using the above methods it is therefore possible to determine required and critical over-pressure versus depth for the removal process of a suction caisson. With these methods the removal process of the suction caisson can be planned and if safe extraction by overpressure is not possible, determination can be made for the amount of additionally needed pullout capacity to be provided by a winch.

3.3 Computer Programs

From the analytical method presented in Subsections 3.1 and 3.2, critical and required under and over-pressures can be calculated versus depth. A plot of this data can then be used in the field to verify measured pressure in the suction caisson while it is being installed into the seabed. To create an accurate plot of pressure versus depth it is necessary to calculate pressure at numerous depths. With multiple calculations required

per caisson installation and the existence of multiple caisson configurations it became necessary to develop a computer algorithm to minimize calculation effort. This algorithm would be used to rapidly calculate pressures at multiple distances, equally spaced, over the entire installation or removal depth for any prescribed caisson configuration.

The following is a description of the algorithms operations. The required inputs for computer algorithm include; vertical step side, caisson geometry, and soil properties. Current caisson embedment is calculated from previous depth and the vertical since. Plug heave is calculated from caisson geometry and current embedment depth to determine the height of the soil plug. Plug height, embedment depth, caisson geometry, soil properties and then used to calculate required and critical pressures. Pressures are stored alongside current height for output. Previous height is then set equal to current height and the process is repeated. These steps are then looped while the soil plug height is smaller than the penetration depth of the caisson. The algorithm is the same for installation and removal. A flowchart of the algorithm for the installation process can be seen in Fig. 3.1.

This algorithm was used to create an installation and removal programs capable of modeling a wide variety of suction caisson configurations. This was achieved by allowing user alteration of caisson shell geometry and by having user input of stiffener area per caisson length. In doing so this program is capable of modeling any cylindrical shelled caisson with any internal stiffener configuration, that provide minimal bearing capacity.

3.3.1 Installation Program

The program *CaissInGenBeta* was created to model the installation process of the suction caissons. It was written in MATLAB. The following is a discussion on the operation of the program and its variables.

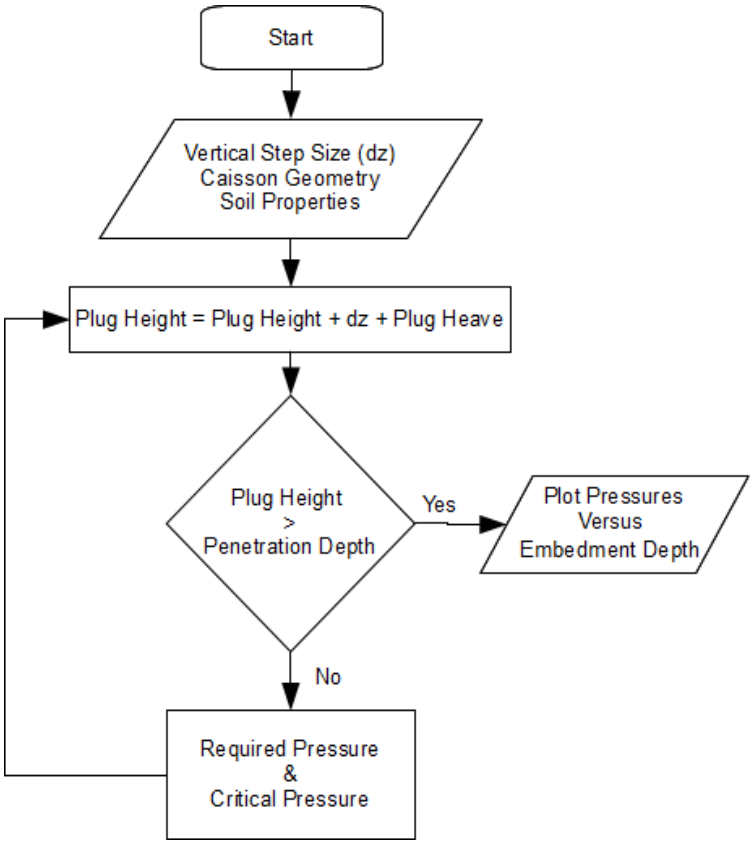

Fig. 3.1: Flowchart of suction caisson installation algorithm

Program inputs are broken into four sections: program traits, caisson geometry, bearing factors, and soil properties. Table 3.1 contains a description of all input variables.

Programs traits are variables that affect the operation of the program, but not the physical state of the model. The user must assign a vertical step size in meters. This affects the number of calculations done per run. A smaller step size requires more calculations which will increase the run time of the program, but also provide higher resolution outputs. The user can also specify a self weight installation depth in meters. Since the required under-pressure during self weight installation is zero it is not necessary for the program to calculate a zero value. The user can estimate the self

weight installation depth and thus reduce the required calculation time. However, if this is over estimated it will impact the accuracy of the solution. Lastly the user can specify file names for saving specified results in text files.

Caisson geometry includes all the physical properties of the suction caisson. The program does not use stiffener geometry as an input. Instead it requires stiffener surface area versus height to be read in as a delimited text file. Column one contains caisson height (m) and column two contains stiffener surface area (m^2). Stiffener area in row one is assigned for zero to height in row one. For all other rows; stiffener area in row i is assigned to heights in rows i minus one to i. The datum for height is the caisson tip. Depth incrementation in the stiffener area input file need not match the vertical step size used in the overall penetration calculation.

User supplied bearing factors include Nc and Nq. They are the bearing factors derived for Terzaghi's bearing capacity equation.

Soil properties are listed in Table 3.1. For this program a linear strength profile is assumed with an intercept at the mud line, Su0, and a shear strength then increases gradient, k.

The main program is broken into multiple sections. Each is organized by what is being calculated. The following will go through each section describing the calculation process.

The simple calculations section includes the preliminary calculations that only need to be completed once. These include the area of the caisson tip, the internal area of the suction caisson, (this is also the area of the soil plug), the submerged unit weight of the soil, the adhesion factor, and the initial plug heave (assuming self weight settlement). In this section a function handle which describes the linear variation of soil strength with depth was also initialized. Use of a function handle will enable MATLAB to integrate the function later in the program.

Table 3.1: Program input variables for *CaissInGenBeta*

Program Traits	
dz	Vertical step size (m)
StartD	Starting depth (m)
Filename1	File name for delimited text file output of required under-pressure versus embedment depth
Filename2	File name for delimited text file output of factor of safety versus embedment depth
Filename3	File name for delimited text file output of critical under-pressure versus embedment depth
Caisson Geometry	
Lf	Length (m)
Lp	Penetration depth (m)
Dout	Outer diameter of caisson shell (m)
Din	Inner diameter of caisson shell (m)
Wsub	Submerged caisson weigth (kN)
Stiff	File Containing stiffener area (m^2) versus depth (m)
Bearing Factors	
Nce	Bearing capacity factor Nc
Nq	Bearing capacity factor Nq
Soil Properties	
Sntv	Sensitivity of the soil
Su0	Soil strength at mud line (kPa)
k	Soil gradient parameter (kN/m^3)
gamma	Soil unit weight (kN/m^3)
Plhe	Plug heave effect variable

The section caisson dz step loop contains a while loop which calculates required and critical under-pressure while stepping over the specified vertical step size. First the vertical step size is added to the current depth. Soil strength at the current depth is calculated. The following resistance forces are then calculated: tip, outer shell, inner

shell, and the stiffener friction.

Stiffener skin friction is calculated by integrating soil shear strength with depth and multiplying by stiffener area over depth. This is looped over the number of stiffener area increments specified in the stiffener area input file, at which point stiffener skin frictional force is summed. As specified previously, the incrementation of depth in the stiffener area file is not limited to the vertical step size. The program is capable of calculating stiffener skin force if the specified vertical size is different than the increments used in the stiffener file. This allows the stiffener area file to be described exactly, leading to accurate solutions without unnecessarily increasing run time.

Once resistance forces are determined the skin friction forces are corrected for adhesion. A statics analysis is then completed to determined required under-pressure. All resistance forces are summed to determine the total force resisting caisson embedment. If this force is less than the submerged caisson weight then the required under-pressure is set to zero. If not required under-pressure is calculated. Once this has been determined the program is able to calculate plug heave, which is dependent on the existence of under-pressure.

Critical under-pressure and factor of safety against blow out are then determined. All calculated forces, pressures, depths, and the factor safety are then stored for possible output. All these variables are listed in Table 3.2. The program then continues to loop until the soil plug height is greater than or equal to the caisson's penetration depth.

The final major section of the program is outputs. The program currently outputs two figures containing plots and three delimited text files. The first figure contains plots of required and critical under-pressure versus exterior embedment depth. The second figure outputs a plot of factor of safety versus exterior penetration depth. Examples of the visual outputs are provided in Fig. 3.2 and Fig. 3.3. The three created text files are of required under-pressure, factor of safety, and critical under-pressure versus exterior embedment depth, respectively. As expressed previously the program stores many quantities as the program loops over the vertical step size. Any person proficient in

MATLAB coding could create outputs of these quantities, as necessary. Though the code does not currently output many of the quantities found in Table 3.2 the capability to do so was included for the convenience of future users.

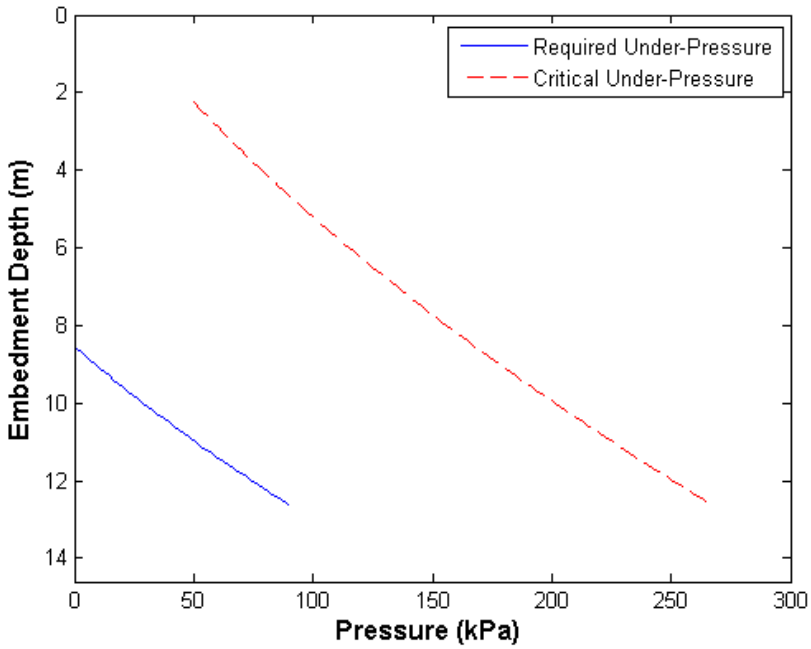

Fig. 3.2: Example pressure output from *CaissInGenBeta*

3.3.2 Removal Program

The second program created was *CaissOutGenBeta,* it was the second program created to model suction caisson physical behavior. *CaissOutGenBeta* models the removal process of the suctions caisson. This program was also written in MATLAB syntax. The following is a discussion on the operation of the program and its variables. To avoid repetitiveness the following discussion describes the removal program comparatively to the installation program.

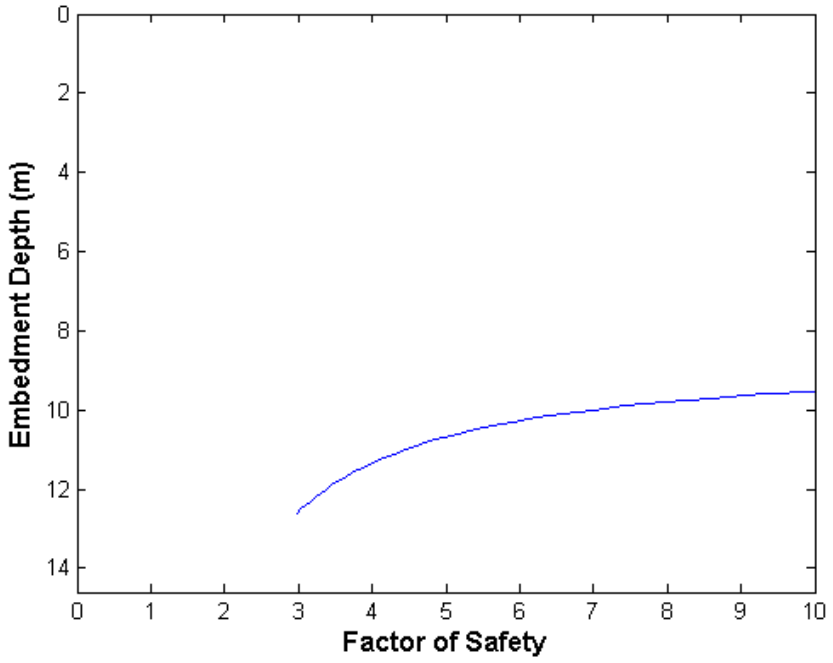

Fig. 3.3: Example factor of safety output from *CaissInGenBeta*

Table 3.2: Variables stored in *CaissInGenBeta* while looping

Stored Variables	
Qtipstr	Force on caisson tip (kN)
Qoutstr	Outside skin friction (kN)
Qinstr	Inside skin friction (kN)
Qplstr	Frictional force on stiffeners (kN)
Qtotstr	Total resistance force (kN)
Qcritstr	Force to cause plug failure (kN)
Prsrstr	Required under-pressure (kPa)
Prsrcritstr	Critical under-pressure (kPa)
zstr	Exterior embedment depth (m)
Zinstr	Soil plug height (m)
Fstystr	Factor of safety

As with the installation program the removal program's inputs are broken into four sections: program traits, caisson geometry, bearing factors, and soil properties. All inputs are the same between the two programs except for the additional input of a winch load, Wnch, and the removal programs lack of Filename2 and Filename3. As noted previously during the removal process a winch is used to apply a vertical force to the caisson as it is removed, so this output must be added. Currently *CaissOutGenBeta* only outputs one file, therefore the input of three file names is not required.

The “main program” of the removal code is the same as that of the installation up to the calculation of resistance forces. Submerged suction weight is included as a resisting force since in lifting the suction caisson, gravity is opposed. The resistance force is then compared to the winch load to determine required over-pressure or lack thereof. Plug heave is then determined once the over-pressure is calculated.

Critical over-pressure and factor of safety against plug failure are then determined. All calculated forces, pressures, depths, and the factor safety are then stored for possible output. All these variables are listed in Table 3.3. The program then continues to loop until the soil plug height is greater than or equal to the caisson's penetration depth.

The final major section of the program is outputs. The program currently outputs one figure containing a plot and one delimited text file. The plot is of required over-pressure versus embedment depth, an example is provided in Fig. 3.4. The created delimited text file contains required over-pressure versus soil plug height. As with the installation program any variable stored in Table 3.3 can be made into an output for the program by any user proficient in MATLAB.

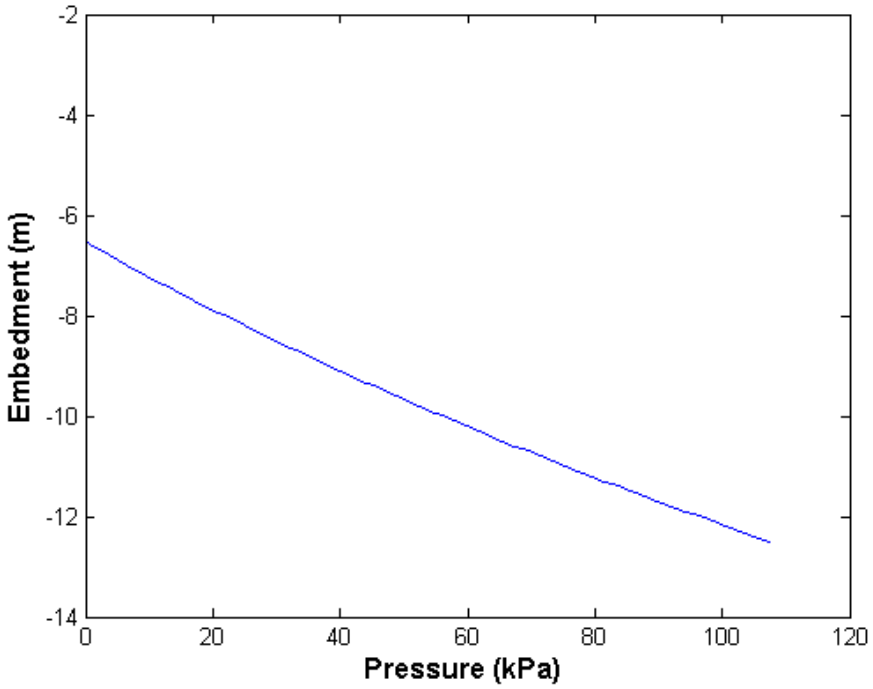

Fig. 3.4: Example pressure output for *CaissOutGenBeta*

3.4 Calibration and Results

The programs *CaissInGenBeta* and *CaissOutBeta* were calibrated using field data provided by Delmar. Included was the data from 20 installations and six removals. Two sites were utilized: 17 installations and three extractions were obtained from the first site and three installation and removal records were from the second site. Delmar used their 21.33m (70ft) suction caissons in these tests, schematics for these suction caissons were also provided. Soil property and strength data was also provided from five exploratory borings, four from the first site and one from the second.

Table 3.3: Variables stored in *CaissOutGenBeta* while looping

Stored Variables	
Qtipstr	Force on caisson tip (kN)
Qoutstr	Outside skin friction (kN)
Qinstr	Inside skin friction (kN)
Qplstr	Frictional force on stiffeners (kN)
Qtotstr	Total resistance force (kN)
Qcritstr	Force to cause plug failure (kN)
Prsrstr	Required under-pressure (kPa)
Prsrcritstr	Critical under-pressure (kPa)
zstr	Exterior embedment depth (m)
Zinstr	Soil plug height (m)
Fstystr	Factor of safety

The field data was used to calibrate the apparent soil sensitivity parameter in the installation and removal programs. It was found that the predicted required under-pressures related to soil sensitivities of two-three best bracketed the installation calibration data. Predicted required over-pressures resulting from soil sensitivities of one-two best bracketed the removal data during calibration. It appears high pore-pressures during the installation process causes increase soil sensitivity. While consolidation effects cause a decrease in the soil sensitivity.

4 EXPERIMENTAL MODELING OF DRAG EMBEDMENT ANCHORS

4.1 Experimental Setup

The goal of the scale model drag embedment anchor testing was to develop a means to record the trajectories of drag embedment anchors with minimal cost and time. It was decided that this could be best accomplished by taking visual measurements with a video camera. To record the trajectory of the anchors in the visible band of the light spectrum it was necessary to develop a transparent testing apparatus to hold the transparent testing medium. The Laponite Tank was developed to fill this need. The Laponite Tank allows the operator to visually record the trajectories of small scale anchors in a transparent testing medium with a video camera.

4.1.1 Laponite Tank

The Laponite Tank testing apparatus is comprised two components: the glass tank and the anchor line guidance system. The glass tank consists of a metal framed box with interior dimensions of 1.8 m (six ft), 1.2 m (four ft), and 0.6 m (two ft). The interior is then lined on the four side walls and the bottom with 1.27 cm (0.5 in) glass plates. The glass plates are attached to each other and the metal frame with caulk. This provided a water proof transparent tank for the testing medium to be held, Fig. 4.1 and Fig. 4.2 the Laponite Tank with interior dimensions of 1.8 m (5 ft 11 in) by 1.19 m (3 ft 11 in) by 0.58 m (1 ft 11 in) and a volume of approximately 1.26 m^3.

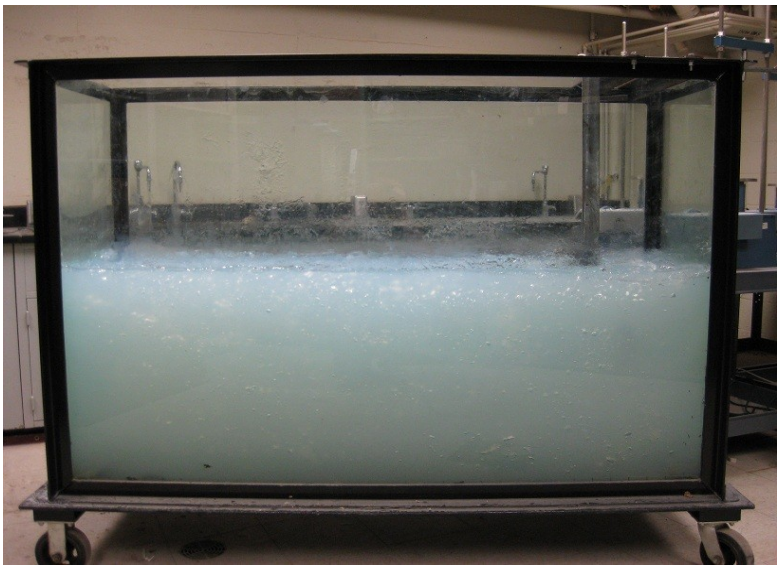

Fig. 4.1: Front view of Laponite Tank with Laponite gel in place

Fig. 4.2: Side view of Laponite Tank with Laponite gel in place

To properly model a variety of field conditions it was necessary to have the anchor line inclination angle at the mudline be changeable between tests. Different anchor line inclination angles are achieved by exerting horizontal force on the anchoring line at different heights above the Laponite gel. Since, the anchor line originates from outside the Laponite Tank it was necessary to develop a guide to redirect the anchor line to said heights. The anchor line guidance system was created by assembling an L-shaped metal frame with pulleys mounted to it, Fig. 4.3. This is then mounted to two metal flat bars that span the top of the tank, Fig. 4.4. The anchor line inclination angle with the mudline can be changed by moving the bottom bracket mounted pulley to any of the nine holes in the vertical bar of the guidance system. The holes are space 5.08 cm (two in) apart, from center. The first hole is located 14.29 cm (5.625 in) below the horizontal bar. This system allows for the user to specify nine different starting anchor line inclination angles. The guidance system can also be attached at different depths along the side of the tank, if necessary.

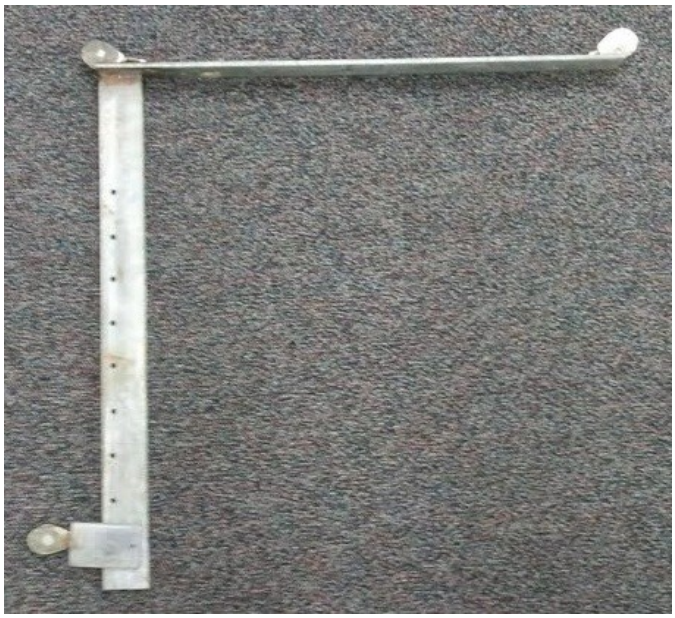

Fig. 4.3: Anchor line guidance system

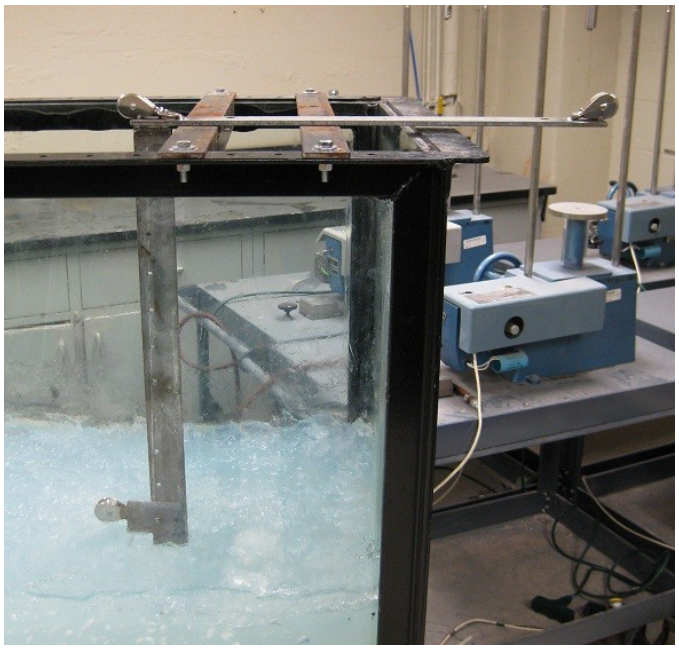

Fig. 4.4: Mounted anchor line guidance system

4.1.2 Anchors and Anchor Lines

Offshore drag embedment anchor flukes have dimensions ranging from one to 5 meters, the Laponite Tank requires scaled anchors. Anchors used in the tank have ranged from 3.8 cm (2.5 in) to 12.5 cm (five in) in size. Anchor size is limited by two factors: trajectory depth and static anchor bearing force. The testing medium in the Laponite Tank has a limited depth. Since larger anchors tend to dive deeper, it is necessary to restrict anchor size in order to prevent the anchor from striking the bottom of the Laponite Tank. Laponite gel also has a low bearing capacity. If the anchor weight is too large compared to its bearing surface area the anchor will simply sink to the bottom of the tank making it untestable. Other than limiting anchor size and weight any anchor configuration should be testable.

For this to be a scaled experiment the anchor line must be scaled with the anchor. There are a number of materials available for use as anchor lines. Metal leader and line used

for ocean fishing were found to be suitable, as they are corrosion resistant and available to a number of sizes. Galvanized wire cable exhibits similar properties. However, there is a final consideration when selecting anchor line. It is also necessary to scale the shackle point connection. If the line is too stiff the connection can be large and impact the anchors trajectory. Anchor lines were connected to a small metal clip by creating a loop and crimping the line to itself using a ferrule or sleeve, Fig. 4.5. The clip then allowed quick attachment and release from the anchor shackle. The main goals in selecting an anchor line is to ensure that the model-to-prototype scale is appropriated; however, it is also important to select a line that will minimize the size of the connection at the shackle point.

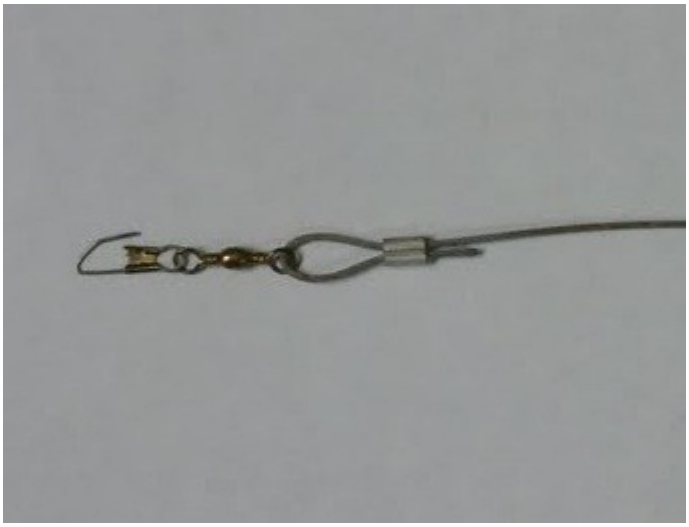

Fig. 4.5: Anchor line connection to be fastened to anchor shackle

4.1.3 Testing Medium: Laponite

The Laponite Tank's name is derived from the testing medium used. The goal of this experimental project is to obtain a visual trajectory of the drag embedment anchor. To do

this the testing medium needed to be translucent, while having enough shear strength to support a static drag embedment anchor. Laponite RD was selected to fill this need. As listed in the technical data sheet provided by Southern Clay Products; Laponite RD is a synthetic layered silicate which forms a gel when dispersed in water as a colloid. At concentrations at or above two percent by weight a thixotropic gel is formed. In the this form Laponite RD is significantly more translucent than soil, Fig. 4.6. However, it is not completely transparent, in large quantities it can be opaque as seen previously in Fig. 4.1. Being a thixotropic gel it is difficult to compare Laponite RD with soils in which shearing results in increase strength.

Fig. 4.6: Translucency of sandy soil (left) compared to Laponite gel (right)

The shear strength of any formulation of Laponite RD is not easily evaluated due to its shear-thinning properties as well as the generally low magnitude of strength. The load range of the geotechnical testing equipment available for this project was larger than the shear strength of the Laponite RD gel. The static shear strength, however, was large to bear the load of the scale anchors tested thus far. Though the shear strength properties of

Laponite gel are not identical to real soils, the observed trajectories were sufficiently similar to those in real soil to permit qualitative evaluations of anchor behavior. To ensure repeatability the tank is covered when not in use to keep water content constant and the Laponite gel was thoroughly mixed 30 minutes prior to anchor testing, with a plus and minus two minute buffer.

The testing medium was created by mixing water with three percent by weight Laponite RD. This was selected based on recommendations from Southern Clay Products Inc. Production of homogenous gels above three percent by weight Laponite RD has been difficult to impossible. Test samples of three, four, and five percent by weight were also created to verify this recommendation. With no measurable or qualitative differences in shear strength the three percent Laponite RD by weight to water was selected to reduce cost and ease formulation.

The Laponite gel was formulated in a batch processing method. Ten gallons of water was mixed with three percent by weight Laponite RD in a mixing basin. The water was mixed with a paint mixer attached to an electric hand drill, Fig. 4.7, as Laponite RD was slowly added to the water. The mixing arm was oriented deep in the water and the mixer was kept at slower speeds to prevent cavitation. Cavitation results in bubbles forming in the gel impacting translucency. The gel was then moved to the Laponite Tank. This process was continued until the Laponite gel was at a depth of approximately 61 cm (two ft) in the tank. The total volume gel is approximately 0.68 m^3 (24 ft^3) in the tank.

4.1.4 Embedment Rate

It is not possible to maintain a constant rate of embedment in the Laponite Tank. To embed the anchor the user must manually pull on the anchor line. The addition of an electric motor would allow embedment to occur at a constant rate of displacement or at a constant force. The data acquisition method however does allow the embedment rate to be determined after testing is complete.

4.1.5 Video Capture Method

Experiments conducted in the Laponite Tank are recorded with a video camera. A

consumer 29 fps analog camcorder was used for recording data. Any video camera can be used for recording the experiments however, higher resolution cameras will allow for better results.

Fig. 4.7: Electronic hand drill and paint mixer used for Laponite gel formulation

To maintain repeatability the floor was marked for camera placement, a tripod was used to support the camera, and a frame was outlined on the tank. Video cameras capture sequential images of the three dimensional world onto two dimensional plans. To make direct comparisons between objects in two different videos they must be at the same distance from the camera. By placing the tripod on the floor markings the data from any experiment can be directly compared. This set up can be seen in Fig. 4.8. However, even though a direct comparison is possible, scale is still lost when using a camera. In order to apply units of length to the data with in a image one known reference length is required, if said length unit is parallel to the image. The frame outlined on the tank allows for a minimum of two reference lengths: its height of 61 cm (two ft) and length of 1.2 m (four ft), Fig. 4.9. With the frame's reference lengths the tripod and floor markings are purely redundant and not necessary.

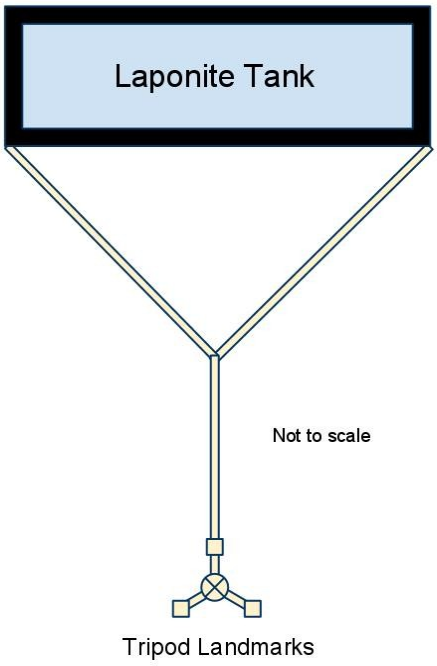

Fig. 4.8: Schematic of landmarks for tripod, with tank as reference

Fig. 4.9: Tank with reference frame

Filming was started prior to the beginning of any experiment and ended after completion to ensure the full experiment was recorded. It was not necessary to record the duration of the experiment while filming since video inherently measures time. With the digitized data any frame can be set as the datum for time equal to zero and time then elapses at a set rate of 29 fps as dictated by the video camera. If another other camera were to be used, such as a high speed camera time would proceed at the frame rate set by the manufacturer.

To provide greater contrast between the Laponite gel and the anchor, flood lights are placed behind the Laponite Tank. Four 500 watt floodlights are used. This results in the anchor appearing darker on film. This is a result of the anchor blocking the light completely while the gel allows a significant amount to pass through. All other lighting in the room is also turned off to prevent contamination.

4.2 Visual Tracking Method

Given the translucent testing medium and tank the simplest way of determining the trajectory of the drag embedment anchor is to do so visually. By locating the anchor on the images taken by the video camera, a trajectory could be measured. It can then be scaled to actual coordinates using a known reference length in the images. This process is labor intensive as the video was recorded at 29 fps and test typical were 25 to 30 seconds. To minimize data processing time a suite of computer software was developed to process the video and provide the anchor trajectories.

The software suite was broken into four programs. First a commercial video processing program converted the analog camera output into a digital format and divided its frames into individual images. Second an image contrasting and thresholding program *AnchThresh* was developed to filter noise out of the images. Third a pattern recognition and location program *LoctAnch* was developed to locate the anchor in each image. Fourth and finally a batch processing program *AnchTrack* was developed to sequentially process all the images from a single video, using the second and third programs, and output the data.

4.2.1 Video Processing

Video processing software is necessary to upload analog video to a computer and to divide the individual frame of the video into separate images. If a digital video camera is used for recording the experiments, the camera will be capable of directly uploading digital footage straight to a computer. Analog digital cameras cannot do this. The output of an analog video camera must be played back through an analog to digital converter attached to a computer with video processing software capable of recording from a source. Analog to digital convertors and video processing software are available as consumer products.

Typical consumer camcorders have a frame rate of 29 fps. That is the camera takes 29 images a second. To track the anchor through the video it is simpler to process the frame as individual images. Therefore it is necessary to break the video's frames into individual images. Most video processing software has this capability. To provide higher contrast images for the data processing the video should be deinterlaced before it is separate into images. Interlaced video provides a better quality video at slower frame rates by combining and blurring adjacent frames. Interlaced images are not recommended because there may appear to be two anchors instead of one in the image.

4.2.2 Image Contrasting and Thresholding

As described in Subsection 2.4.1 grayscale images are simply visual representations of a two dimensional matrix with entry values between zero and one. The image contrasting and thresholding program takes a grayscale image of the Laponite gel with the embedded anchor and converts the entry values for the gel to one and the entry values for the anchor to zero. Visually this will make the gel white and the anchor black. This creates extreme contrast between the anchor and the gel making to easier to locate. This processes however is not simple. The Laponite gel contains numerous shades of gray many darker than the anchor model. To have the computer isolate the anchor from the background noise in the Laponite gel a number of image processing techniques are used.

The image contrasting and thresholding program *AnchThresh* was developed to create a

binary of the anchor isolated from the background. Background removal algorithm involves multiple step. First a ten pixel by ten pixel median filter is applied to the original image, example in Fig. 4.10, resulting in Image A, Fig. 4.11. This removes the salt and pepper noise. For images collect from the Laponite Tank the salt and pepper noise is a resultant of the shadows cast by bubbles in the gel. Applying the median filter will prevent individual noisy pixels from distorting the image when the averaging filter is applied. The original image is then passed through a small averaging filter, 15 pixel by 15 pixel, to remove any distinct noise in the background and then sharpened creating Image B, as in Fig. 4.12.

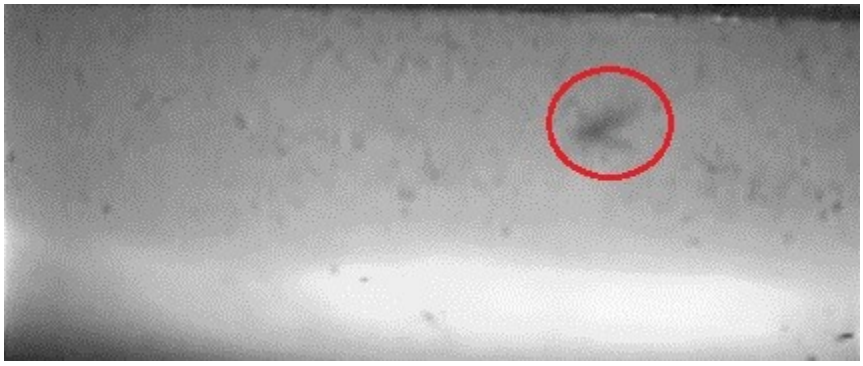

Fig. 4.10: Example original image passed to *AnchThresh* with anchor circled in red

Fig. 4.11: Image A, result of median filter

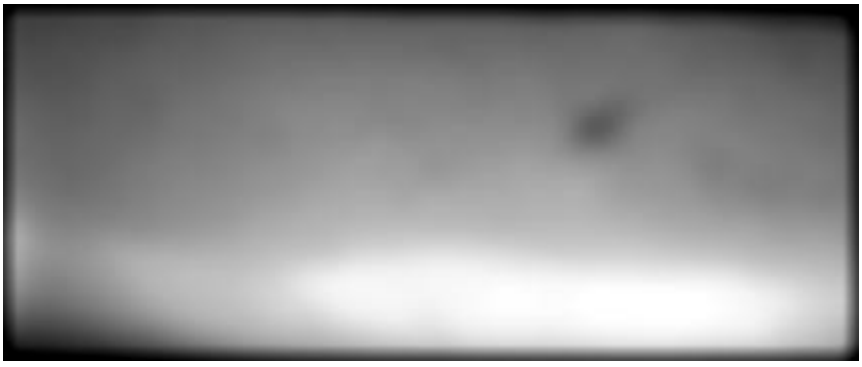

Fig. 4.12: Image B, result of small averaging filter

The Image A is then also passed through a large averaging filter, 65 pixel by 65 pixel, to blend the image of the anchor into the background, essentially removing the anchor from the background, as seen in Fig. 4.13, creating Image C.

Fig. 4.13: Example of Image C with anchor removed by large filter

The Image C is then inverted and added to Images B and then sharpened, resulting in Image D seen in Fig. 4.14. This results in a lightening of the dark areas in the background specifically near the edges, but not on them.

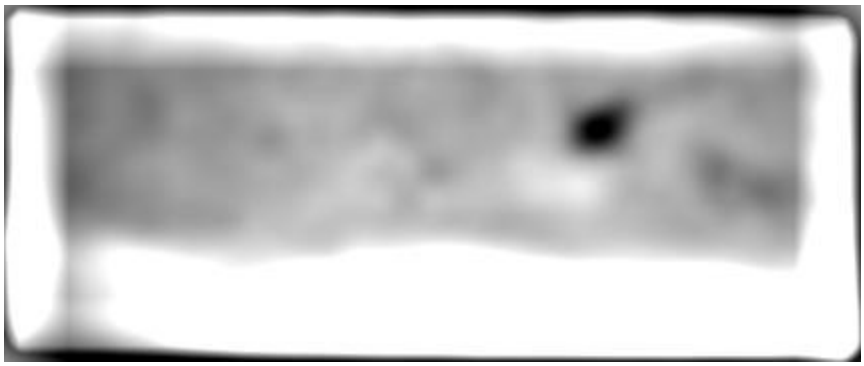

Fig. 4.14: Example of Image D with background partially removed

Image D is then added to Image A to remove the remaining portions of the background and sharpened to create Image F seen in Fig. 4.15.

Fig. 4.15: Image F with the majority background removed

An edge removal filter is then added to Image F to remove the dark edge created as a resultant of the averaging filters. Creating Image G as seen in Fig. 4.16. The edge removal filter is created by applying the large averaging filter to a white image the same size as the original image. The image is then inverted, thresholded, and converted back to grayscale. The final grayscale conversion allows the image to be used in mathematical operations with other grayscale images.

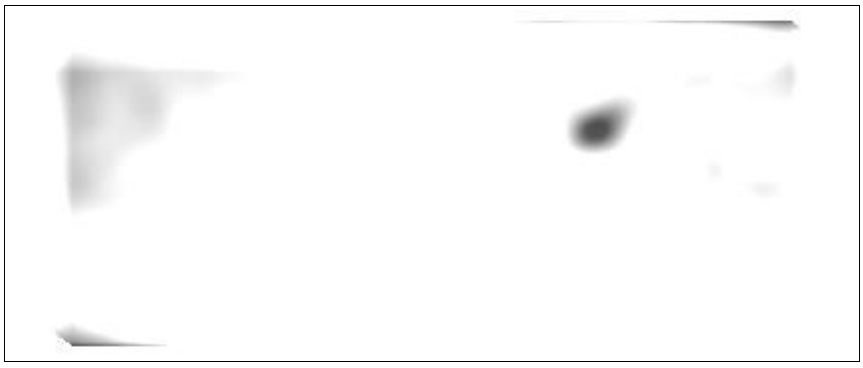

Fig. 4.16: Image G with edge filter applied, border added for clarity

Image G this then converted to a binary image where the background is white and the anchor is black, Fig. 4.17. This binary image will be passed to the pattern recognition program to locate the image of the anchor.

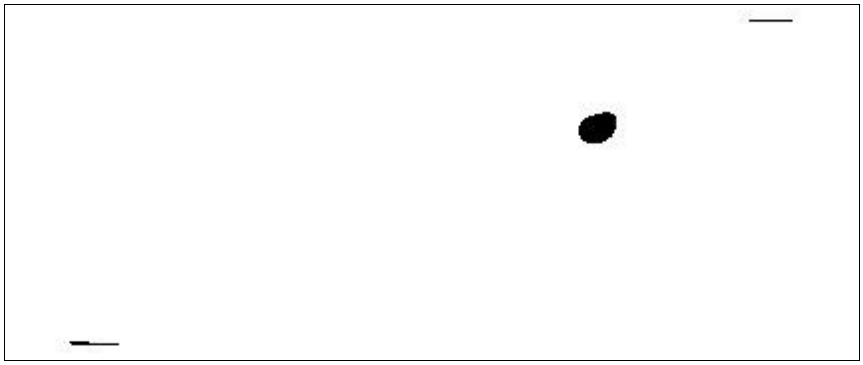

Fig. 4.17: Final binary image, border added for clarity

The program *AnchThresh* was created in MATLAB utilizing its the available image processing tools. In MATLAB terminology this script is a function. The function has two inputs and one output. It requires an input of a grayscale image and a threshold variable. It outputs a binary image. A list of the primary MATLAB image processing functions used in AnchThresh has been provided in Table 4.1.

The first step in the function is to initialize the two averaging filters. This is done with the *fspecial* function. As noted above the small averaging filter is 15 pixels by 15 pixels while the large filter is 65 pixels by 65 pixels.

The function then goes through the process of creating the edge removal image. A white image is created using the size of original image and the *ones* function. The large averaging function is then applied to the white image using the *filter2* function. The image is then inverted with the *imadjust* function. That is the *imadjust* function is used to

map the color black (value zero) to the color white (value one) and vice versus. The image is then threshold using the *im2bw* function with a level of 0.4. The image is then converted back to grayscale using the *mat2gray* function.

Table 4.1: MATLAB functions used for image processing in *AnchThresh*

Function	Description
fspecial	Initialize two dimensional filters, such as averaging
filter2	Applies two dimensional filter to image
imadjust	Adjust grayscale levels in the image, can be used to invert an image
imadd	Sums two images together to create a third
im2bw	Thresholds an image based on selected grayscale value
graythresh	Predicts a grayscale value for use in *im2bw*
mat2gray	Converts a matrix to a grayscale image

The function then proceeds to edit the input image. The median filter is applied to the original image using the *medfilter2* function, as noted above this is a 10 pixel by 10 pixel mask, creating Image A. The large and small filters are applied to image A using the *filter2* function creating Images B and C respectively. Image B is then sharpened using the *imadjust* function. Image C is inverted with the *imadjust* function resulting in Image D. The MATLAB function *imadd* is used to sum Images D and B creating Image E. Image E is then sharpened. Images E and A are then added together to remove the rest of the background using the *imadd* function, this produces Image F. Image F is sharpened and then summed with the edge removal image created previously, resulting in Image G. Finally the output binary image created by thresholding Image G with the function *im2bw.*

While thresholding Image G user desecration is necessary. The function *im2bw* requires a threshold level as an input. The MATLAB function *graythresh* attempts to predict this

value. However, its results have not been found sufficient. If the background has not been fully removed, the level predicted by *graythresh* can eliminate the anchor from the image. A threshold variable has been added to the code in order to adjust the level. The threshold variable is a required input for the function *AnchThresh*, via the caommand prompt.

The final binary image of the anchor will be passed back to the program which ran the function *AnchThresh*.

4.2.3 Pattern Recognition and Location

The program *LoctAnch* was developed to locate the anchor in a binary image. The binary image passed to *LoctAnch* contains the anchor in black and the background in white. However, the process of removing the background is not perfect and a small amount of noise is left. Therefore the program must distinguish between the anchor and the noise. *LoctAnch* is a program which receives a binary image and a limiting frame size, recognizes the anchors from the noises, and outputs the x-y coordinates of the anchor in pixels.

The ultimate goal of *LoctAnch* is to determine the x-y coordinate of the anchor. The only means of doing this is to scan through the array entry by entry until a group of zeros is located. However, as seen in Fig. 4.17 the *AnchThresh* does allow a small amount of noise to be left in the background. To ensure that noise is not mistaken for the anchor, only the anchor can be visible in the image that is scanned. *LoctAnch* does this by cropping the image until the length of the longest side is less than four times the shank length in pixels. It is assumed there will be no noise within this area because of the contrast provided by the anchor.

The program *LoctAnch* also operates on the assumption that the number of pixels that make up the anchor will be greater than the number of pixels in the noise, in an area equal to half of that of the image. This is utilized by dividing the image into three images each of which are half the area of the original image. The image is first divided in half then a third image is oriented over the center, as seen in Fig. 4.18. Based on the previous

assumption the image with the most black pixels will contain the anchor and since binary images are arrays with ones designating white and zeros designating black; the array with the lowest mean value will be the one containing the anchor.

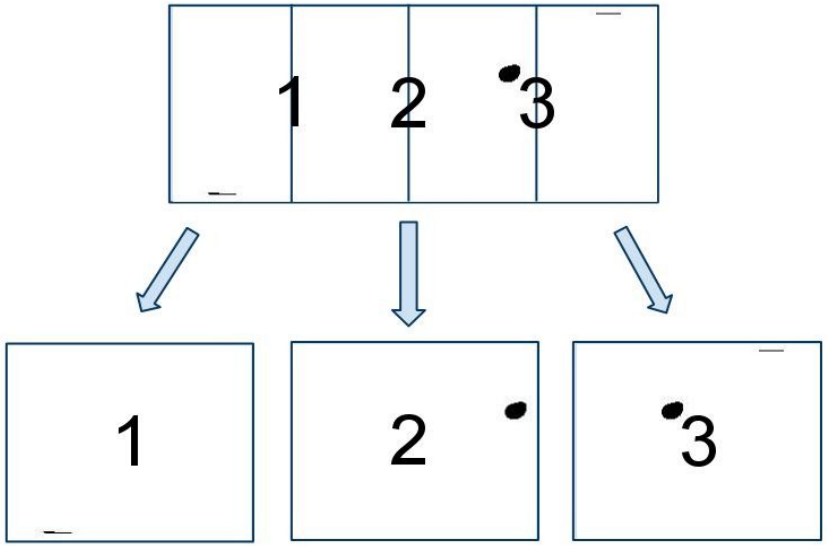

Fig. 4.18: Division of binary image into three images, borders added for clarity

In the example provided in Fig. 4.18 the image with the lowest mean value will be Image 3. Though Image 2 also contains the anchor number three the noise in Image 3 reduces the mean value of the array. An image that contains the anchor and noise will be preferred over an image with only an anchor. This is the second reason to reduce the image size before scanning it entry by entry as mention above.

Image reduction then continues by dividing Image 3 into three parts each with areas equal to half of the Image 3. The mean is once again taken and the processes is continued with the selected image. The program *LoctAnch* will do this until the length of the longest side of the image is less than four times the shank length in pixels, as mentioned before. An example of the final image is seen in Fig. 4.19. This processes is not limited to division in the horizontal direction. The program will make divisions along the longest edge.

Once the image has been reduced to the proper size the program will scan the image array entry by entry until the zero values are found. The anchor's location is then designated by the pixel closest to the left edge. In most cases this will correspond to the fluke shank intersection of the anchor, under normal operation.

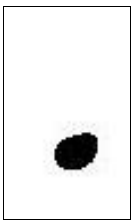

Fig. 4.19: Example of final cropped image, border added for clarity

LoctAnch was created in MATLAB. In MATLAB terminology this script is a function. The two required inputs for the function are a binary image and maximum final image length. The function outputs a one by two array containing the x-coordinate and y-coordinate respectively in pixels. The origin of the Cartesian coordinates is located at the top left of the original image. The x-axis is positive to the right and the y-axis is positive down.

The function *LoctAnch* follows the previously presented algorithm using basic MATLAB array operations and will not be detailed further. However, the following should be noted. The function makes divisions along the rows first then proceeds to divided the image along the largest side. Also, To expedite the entry by entry scanning process *LoctAnch* only finds and stores location of the first zero value in each row. If there are no black pixels in the row it stores a default values of 1000.

4.2.4 Batch Processing

The MATLAB functions *ThreshAnch* and *LoctAnch* can process a single image effectively. The background is removed and the x-y coordinates of the anchor is located in pixels. However, they can only process one image at a time. With a frame rate of 29 fps and approximately 25 seconds per experiment there can be a maximum of 725 individual images available for processing. Running these images one at a time would be an extensive and avoidable time sink. The program *AnchTrak* was developed to batch process the images. *AnchTrak* serves as the means of organizing all the necessary input data, running all of the images from a single experiment through the functions *ThreshAnch* and *LoctAnch* and outputting anchor trajectory in multiple formats.

The program *AnchTrak* imports all of the images into the program to be processed by itself. This is done by utilizing a standard file naming system. All files need to have a generic file name, usually indicative of the experiment parameters, followed by a numeric value indicating sequence. By inputting the generic file name and the number of images to be loaded the program can read all of the images. A starting image number can also be assigned. The first image to read will be that with the indicated number. This is helpful to reduce the processing time if there are a number of images where the anchor is not visible.

To convert from pixels to real world coordinates a number of pixels must be set to a reference length. The reference length comes from the length of the reference frame on the Laponite Tank. To relate this length to pixels a graphic user interface (GUI) is called in *AnchTrak* to measure the number of pixels in the reference frame, within the image.

The GUI, which is a built in MATLAB function, allows the user to place the endpoints of a line anyplace of a image and measure the number of pixels in between, as seen in Fig. 4.20. A ratio number of pixel over reference length will allow the conversion from a distance in the image to a distance in the real world.

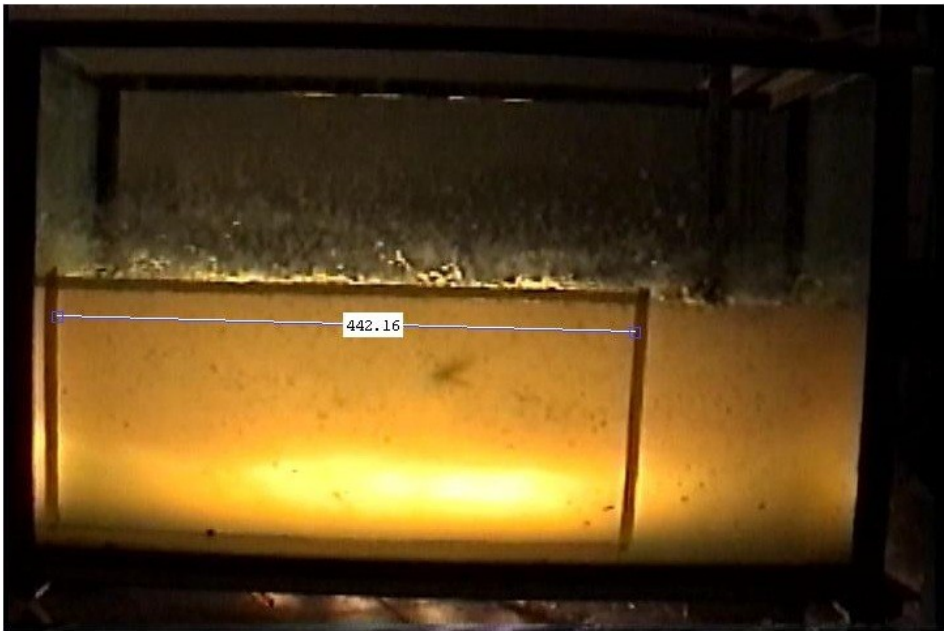

Fig. 4.20: MATLAB pixel measurement GUI with example Laponite Tank image

To aid the image contrasting and thresholding process, it is necessary to crop the image around the reference frame affixed to the Laponite Tank. When the experiment is recorded the images may contain the entire tank. The function *ThreshAnch* was designed to remove the background from an image which contains only the anchor and Laponite gel. *AnchTrak* calls up a GUI cropping tool. In the GUI the user must crop within the reference frame, this is shown in Fig. 4.21. The cropped image is shown in Fig. 4.22. The top left corner of the crop tool will become the origin of the axis system. It is only

necessary to crop one image. The cropping tool saves the cropping coordinates to a variable which can then be applied to the rest of the images.

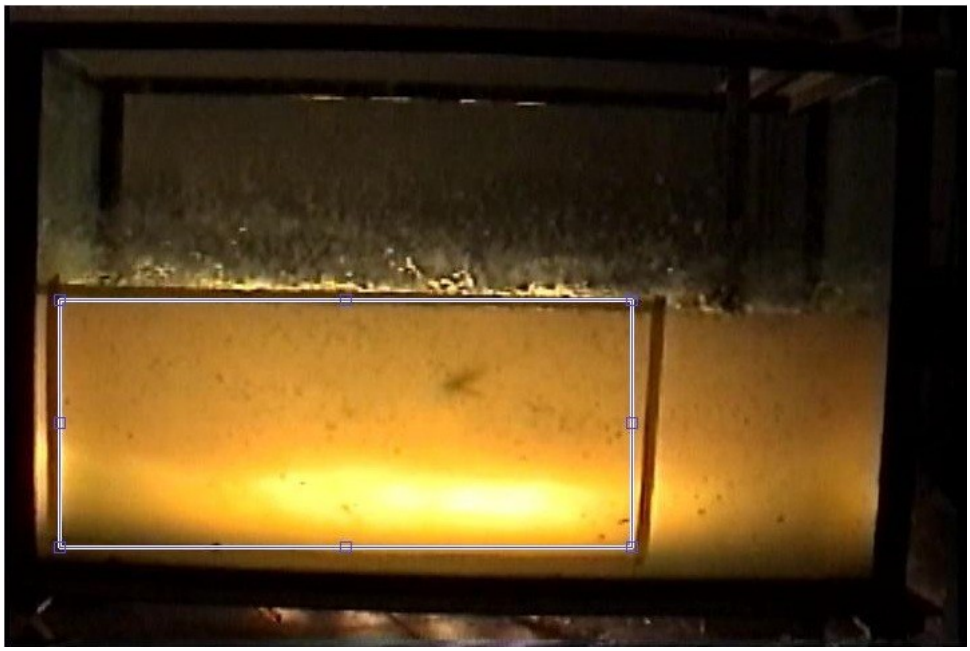

Fig. 4.21: MATLAB image cropping GUI with example image

The program then uses the physical length of the experimental anchor and the ratio of pixels to reference length to calculate the final image length for *LoctAnch*. By experimentation it was discovered that a maximum image length of four time the pixel length of the experimental anchor is sufficient. This is calculation is editable in the script by the user, however it is necessary to take into account the information outlined in Subsection 4.2.3.

The program *AnchTrak* then proceeds to test thresholding variables. The thresholding variable is used by *ThreshAnch* to convert the background-less anchor image from grayscale to binary. This value is affected by the level of noise in the original image. If

the wrong value is used there can be too much noise in the image or the image can be blank The program selects images half way and three quarters of the way through the sequence. These images are converted to binary with the user inputted threshold values and displayed. The user is then given the option to keep the threshold value or edit it. This process is looped until the user is satisfied. This type of user control in *AnchTrak* attempts to prevent the program from providing null results.

Fig. 4.22: Example cropped image from GUI

The program then begins batch processing. The program sequential sends all of the desired images through the function *ThreshAnch* and *LoctAnch*. This process is done with a loop. The first image is read converted to a grayscale image and cropped using the coordinates designated from the cropping tool earlier. This image is then sent to the function *ThreshAnch* where the background is removed and the image is converted to binary. The binary image is then sent to the function *LoctAnch* where the anchor is located and the coordinates are passed back to *AnchTrak*. The coordinates are then stored to be outputted later.

Before the process is looped and next image is read, *AnchTrack* decides whether to use

the binary image for a time lapse picture. The program outputs a time lapse image of the anchor's trajectory. This image is built using a time lapse variable. This sets the frequency of images used in the composite image. If it is set to 25, one in 25 images will be used. To create the time lapse image the binary images are simply added to each other. This helps by providing a visual representations of the experiment in a single image, example provided in Fig. 4.23. It also provides a measure of experimental and image processing quality.

Fig. 4.23: Example time lapse image

The program *AnchTrack* then proceeds loop the above process reading in the images sequentially storing the coordinates and creating the time lapse image. The program finishes by outputting the final time lapse image as a Tagged Image File Format (tiff), Fig. 4.23. It also outputs the coordinates of the anchor in a tab delimited text file. The coordinates are written as x and y respectively and as mention previously x is positive right and y is positive down.

The program *AnchTrack* was written in MATLAB. The program has 13 required user inputs and two outputs. It also requires the use of two custom functions. These functions

are *ThreshAnch* and *LoctAnch*. They have been outline previously in Subsections 4.2.2 and 4.2.3 respectively. The program take images, from experimentation in the Laponite Tank, as inputs and outputs anchor trajectory.

There are thirteen required inputs for the program *AnchTrak*. The required inputs are listed in Table 4.2. Inputs are broken into three types: physical properties, image properties, and file properties. Physical properties relate the image to experimental dimensions, these include length of the reference frame attached to the Laponite Tank and shank length of the test anchor. Units are not specific although they need to be consistent. Image properties include the number of images to be processed, the first image to be processed, the thresholding variable, and the time lapse variable. File properties include file names and directory names for the location of the images and output files.

The program AnchTrak uses standard MATLAB operations and functions. The program follows the algorithm presented above and the majority will not be further outlined. Image processing programing techniques and functions in MATLAB will be discussed.

The MATLAB function *imdistline* is the GUI used to measure the distance of the reference frame in pixels in the image of the Laponite Tank. This function requires a figure and an axis. The function outputs information into a handle. The function *getDistance* is used to retrieve the length of the measurement tool from the handle.

The MATLAB function *imcrop* is the GUI used to crop the image of the Laponite Tank. The function's minimum required input is an image. The function outputs an array of a cropped image and cropped image coordinates, respectively. The coordinates can be used as a second input for *imcrop*, adding the second input will eliminate the GUI.

As described in Subsection 2.4.1 there are two ways to describe grayscale images: one, gray intensity is described with the integer values of zero to 255 or two, grayscale values are described as fractional numbers between zero and one. The MATLAB function *rgb2gray* converts a color image to a grayscale image with entry values of zero to 255. The MATLAB function mat2gray converts any matrix to a grayscale image with entry

values of zero to one. For the program *AnchTrak* all image processing conducted on grayscale images was programed for entry values of zero to one.

Table 4.2: Inputs for *AnchTrak*

Physical Properties	
Length	Length of reference frame
Shank	Anchor shank length
Image Properties	
n	Number of images to be analyzed
n2	First image to be analyzed
Thv	Threshold variable, 0-0.3 recommended
Tlps	Time lapse variable
File Properties	
Filename1	String with generic name of the image to be analyzed
Fileext1	String with file extension
Filename2	Name for output textfile
Filename3	Name of saved time lapse image
Direct1	Output directory
Direct2	Input Directory
Direct3	Directory with software and functions

4.3 Parametric Study and Results

A number of experiments were conducted in the Laponite Tank. The first experiment was conducted to examine the effect the thresholding variable has on measured anchor trajectory, during data processing. For this experiment only a single test was conducted. A second series of experiments was conducted to test the effect of anchor line diameter on anchor trajectory. For this series 15 drag embedment tests in the tank were performed. Finally the effects of out-of-plane loading during installation were examined. For this

test series, four embedment tests were conducted.

4.3.1 Interpretation of Results

Prior to the presentation of results, it is necessary to discuss how results are interpreted from experiments conducted in the Laponite Tank. As noted before in Subsection 4.1.3 the selection of Laponite gel as a testing medium was due to it's translucent properties and bearing strength. The translucency of the testing medium allows the anchor's trajectory to be recorded with a camera. However, as stated before the shear strength of the gel could not be measured, with available testing equipment and the gel has thixotropic properties. Attempting to make quantitative comparisons between experiments conducted in the Laponite Tank and soil is not feasible.

While quantitative comparison were only made between tests conducted in the Laponite Tank; it is possible to make qualitative comparisons between tests conducted in the tank to those in the field. A test with a specific anchor should never be used to predict embedment depth in soil. However, relative comparisons of embedment depths from the Laponite Tank tests for various anchor types can be considered meaningful.

The Laponite Tank provides the ability to see the trajectory of an anchor. This is an invaluable capability. This ability also limits the extrapolations experimental results to field conditions. The tank can still serve as a practical tool if it is used in the correct context.

4.3.2 Parametric Study of Threshold Variable

The threshold variable is a user assigned variable needed for image processing. The threshold variable is used in the conversion of the experimental image from grayscale to binary. The variable's value will impact the amount of noise that is transferred to the binary image. The threshold variable also has an impact on the size of the anchor in the image. As seen in Fig. 4.24 a large threshold variable of 0.4 results in the anchor being small while a value of 0.2 results in a larger anchor. A evaluation of the impact of this variable on the results was needed.

Fig. 4.24: Time lapse images with threshold variables of 0.2 (left) and 0.4 (right)

A parametric study was conducted on the effects of the threshold variable. A single experiment was conducted in the Laponite Tank. An anchor with an approximate shank length of 8.9 cm (3.5 in), a fluke length of 8.9 cm (3.5 in), and fluke-shank angle of 50 degrees was used. Anchor line diameter was 1.58 mm (1/16 in).

This single test was processed with the program *AnchTrak* five times, with a different threshold variable being used each time. The threshold variable ranged from 0.2 to 0.4 in increments of 0.05. The the trajectories were then plotted in Fig. 4.25 for comparison. The y-axis was exaggerated. Extraneous points indicative of noise in the image were not removed. All trajectories should be identical since the same experimental data was used in each of the five image processing runs. Fig. 4.25 verifies this, there is little variation in the trajectories.

The threshold variable will impact the appearance of the time lapse image with larger values decreasing the size of the anchor. The user however, does not need to be concerned about the threshold variable impacting results. This is assuming that a threshold variable is selected which minimizes noise without totally removing the anchor from the image.

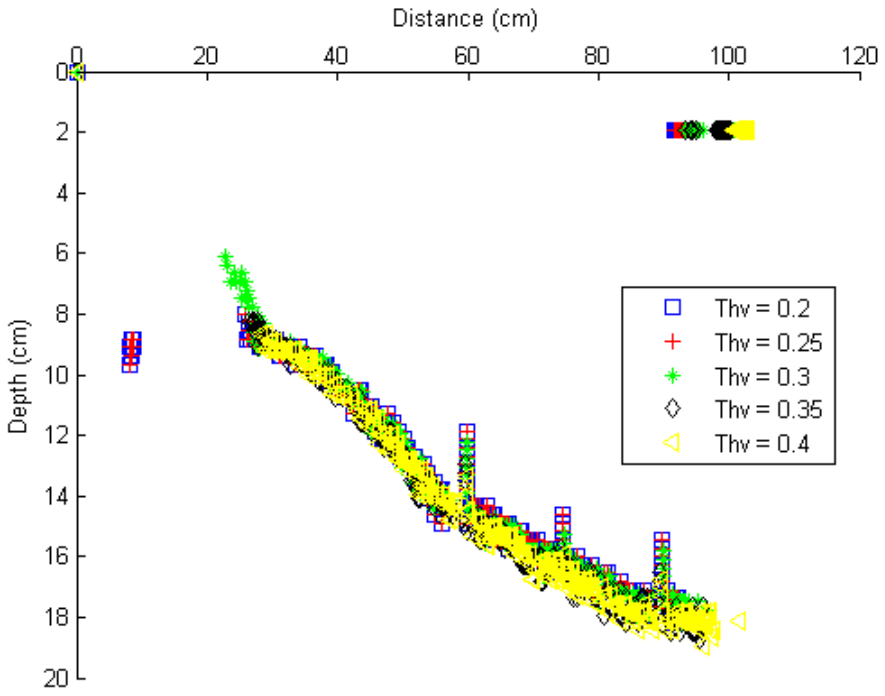

Fig. 4.25: DEA trajectories with variation in threshold values (not to scale)

4.3.3 Impact of Anchor Line Diameter

The effect of anchor line diameter on depth of anchor embedment was examined. As the DEA embeds in the soil the anchor line provides resistance. A large diameter should provided higher resistant forces because of the larger surface area. This was tested in the Laponite Tank. By running multiple tests with the same anchor, but with varying anchor line diameter the trajectories can be examined. Trajectories with larger anchor line diameters should be shallower the others.

Three different anchor lines were used. The diameters of these lines were 0.96 mm, 1.58 mm (1/16 in) and 3.18 mm (1/8 in). Five tests were ran with each anchor line for a total of 15 tests in this experiment. The same anchor was used for all 15 tests. This

anchor has a fluke length of 11.43 mm (4.5 in), a shank length of 11.43 mm (4.5 in), and a fluke-shank angle of 50 degrees. By only varying the anchor line diameter in between the sets of tests their effect can be examined.

All 15 test were conducted in the tank then ran through the image processing software *AnchTrack*. Further data processing was then conducted to remove extraneous data points from the trajectories. These extraneous points are the result of the pattern recognition function confusing the anchor with noise. Their removal is necessary to preform a polynomial regression on the anchor's trajectory.

The extraneous data points were removed by the following custom data processing algorithm. All points shallower than one inch were removed. The shadowing around the surface of the soil tends to hide the image of the anchor resulting in a high amount of noise. Any points displaced further than 0.76 m (2.5 ft) within the first 30 frames were removed. Shadowing from the surface of the Laponite gel tends to result in a smaller anchor image at the beginning of the test, if it is not hidden at all. The pattern recognition program can confuse the anchor with noise in the top right corner of the image. By restricting the points to the left half of the image in the beginning these points are removed. Finally any points that were displaced more than an inch vertically from the next or previous point was assumed to be noise and were removed.

The results from all 15 test are plotted in Figs. 4.26-4.29. The plots in Figs. 4.26-4.28 are trajectories similar anchor line diameter plotted independently, while Fig. 4.29 contains all trajectories plotted simultaneously. In these plots W refers to a diameter of 0.96 mm, C refers to a diameter of 1.58 mm, and V refers to a diameter of 3.18 mm. As seen in these plots the data is scattered and not easily interpreted. A least squares polynomial regression to the fourth power was preformed on the set of data for each different anchor line diameters and plotted in Fig. 4.30, to provide a clearer picture.

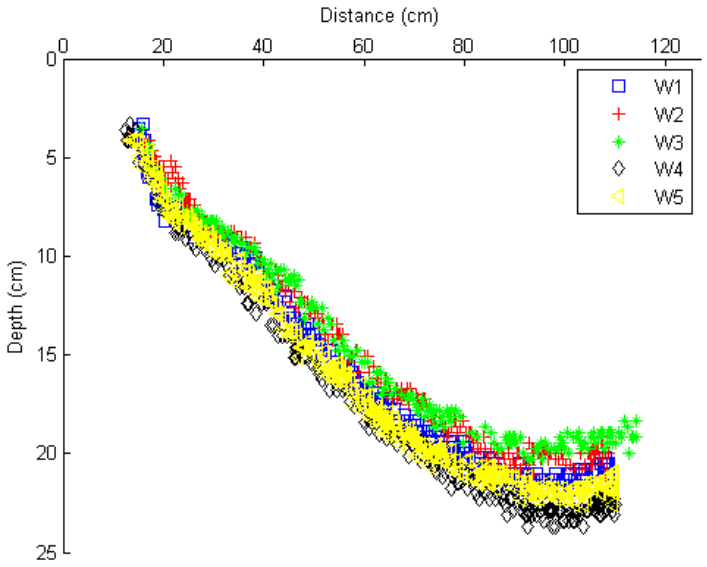

Fig. 4.26: Trajectories for anchor line diameter of 0.96 mm (not to scale)

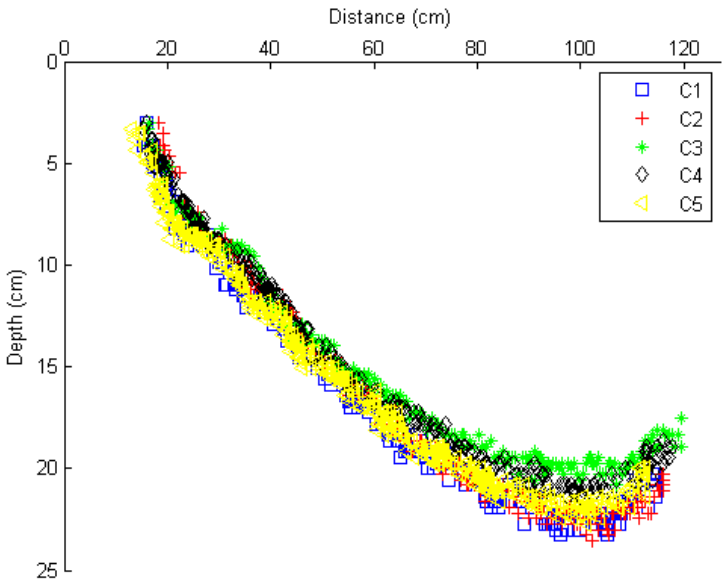

Fig. 4.27: Trajectories for anchor line diameter of 1.58 mm (not to scale)

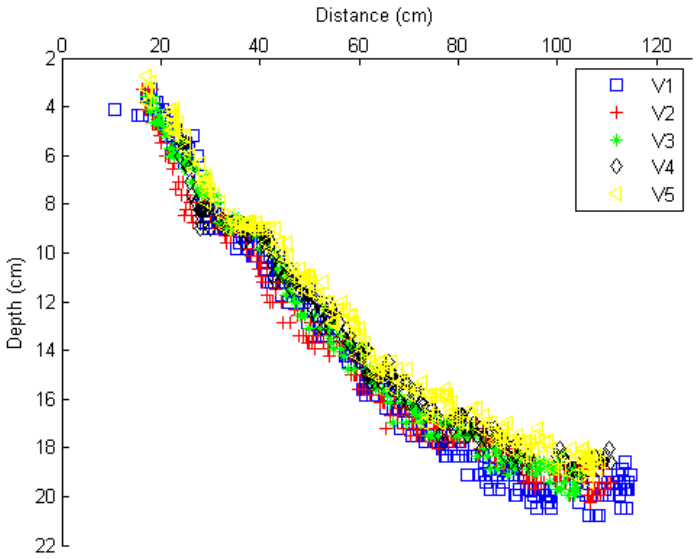

Fig. 4.28: Trajectories for anchor line diameter of 3.18 mm (not to scale)

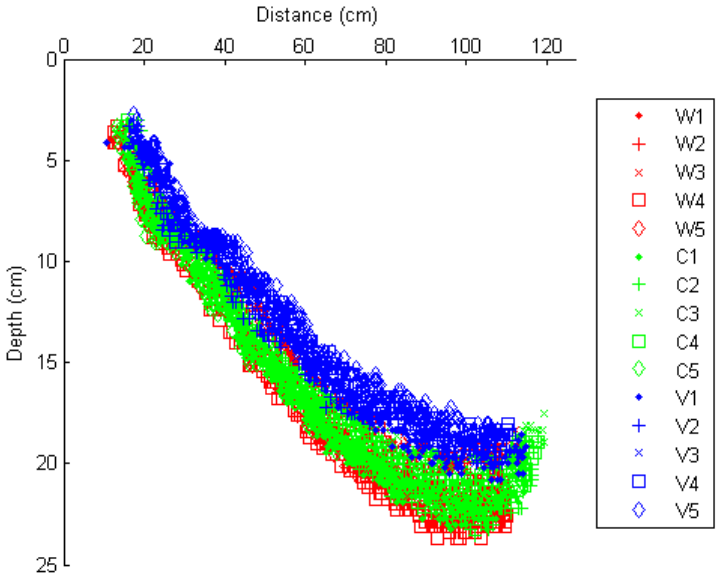

Fig. 4.29: Trajectories for varying anchor line diameter (not to scale)

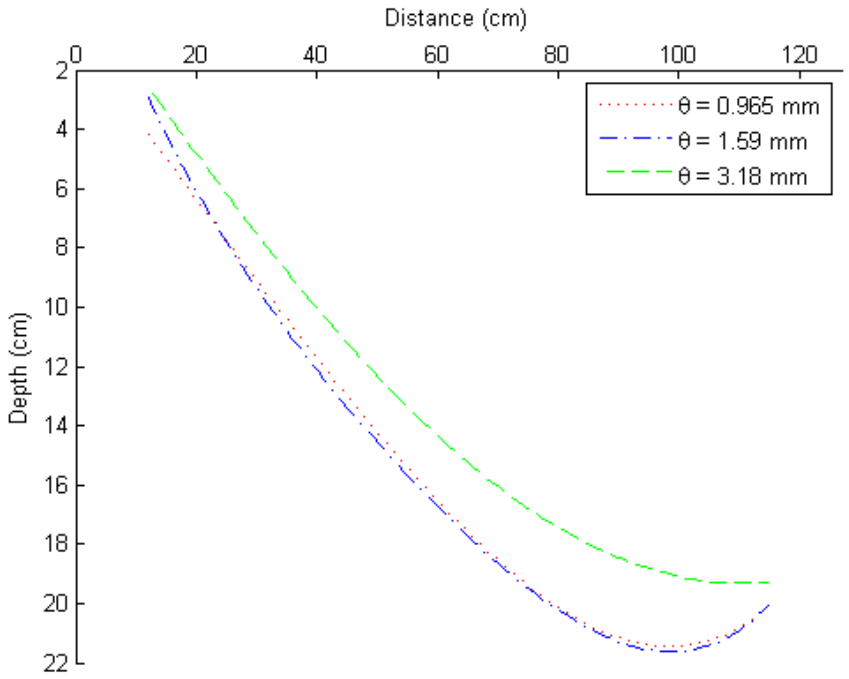

Fig. 4.30: Regression trajectories for varying anchor line diameter (not to scale)

The regression plots in Fig. 4.30 show that anchor line diameter does impact embedment depth. An increasing to an 3.18 mm diameter anchor line from 0.96 mm or 1.58 mm line significantly reduced embedment depth. However, a 64 percent increase in anchor line diameter from the 0.38 diameter line did not produce measurable results. It appears the vertical sampling error, in repeatable test within the Laponite Tank, is larger than the decrease in embedment depth for anchor lines smaller than 1.58 mm inch.

Increasing anchor line diameter increases resistance against the anchor line in the soil resulting in shallower embedment depths. This is supported by experimentation in the Laponite Tank. However, a clearer relationship between DEA embedment depth and anchor line diameter could not be established because of the anchor line sample size and vertical error between repeatable tests in the Laponite Tank.

4.3.4 Impact of Out-of-Plane Loading

Tests were conducted in the Laponite Tank to examine the effect of anchor embedment depth during out-of-plane loading. A schematic of the Laponite Tank is shown for this experiment in Fig. 4.31. Tests were conducted for displacements in the z-direction equla to zero cm, 10.16 cm (four in), and 20.32 cm (eight in) prior to embedment. Three tests were ran for each displacement in the z-direction. The anchor used for this experiment had a fluke length of 11.43 mm (4.5 in), a shank length of 17.78 mm (7 in), and a fluke shank angle of 50 degrees.

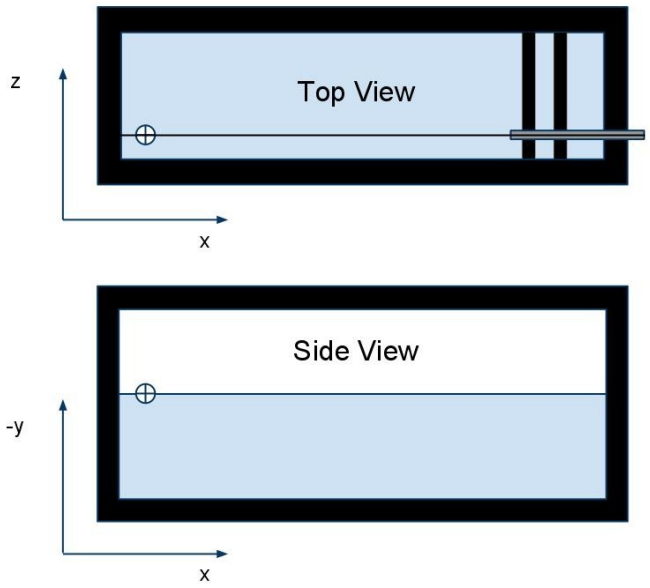

Fig. 4.31: Laponite Tank schematic, origins at cross hairs

Data processing was conducted to remove extraneous points which were the resultant of *AnchTrack* confusing the image of the anchor for noise. Extraneous data points were removed with the following custom data processing algorithm. Any point above and or

before three inches was assumed to be noise and removed. Shadowing from the Laponite surface and the right edge creates noise indistinguishable from the anchor at shallow depths. Finally, any points which is displaced more than an inch vertically from the immediately adjacent points were assumed to be noise and removed.

The trajectories from all nine tests are plotted in Fig. 4.32. Polynomial regressions to the fourth power was used to plot the average trajectories for each set of tests. These were plotted in Fig. 4.33. As seen in the two figures embedment due to out-of-plane loading does impact the anchors maximum depth. Anchors displaced 10.16 cm (four in) out-of-plane did not embed as deeply as those in-plane. Anchors displaced 20.32 cm (eight in) out-of-plane had a final embedment less than those in-plane or four inches out-of-plane.

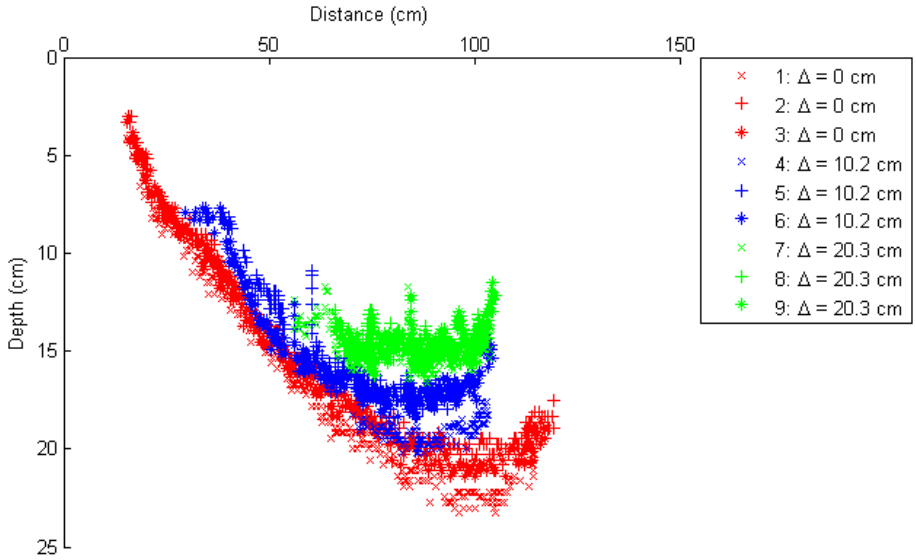

Fig. 4.32: Out-of-plane anchor trajectories

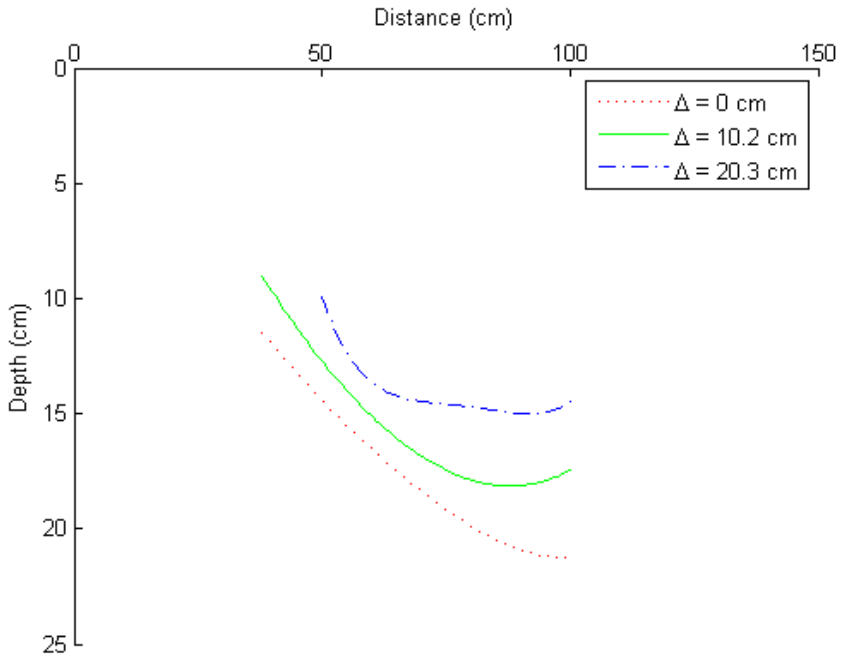

Fig. 4.33: Average out-of-plane anchor trajectories

These results are as expected. This process has been examined in Aubeny and Chi (2010b).When loading out-of-plane the anchor has not only forces in the x-y direction, but also the z. This results in a rotation of the anchor as it moves and a smaller force in the z direction. The resultant is a shallower embedment than an anchor loaded in-plane. Similar results should qualitatively be expected in soil.

5 ANALYTICAL MODELING OF DRAG EMBEDMENT ANCHORS

5.1 Overview

As described in Subsection 2.3.2 an analytical model for describing DEA trajectories is presented in Aubeny et al. (2009). This analytical method provides as a means of qualitatively verifying the data obtained in the Laponite Tank. As stated in Subsection 4.3.1 data obtained in the Laponite Tank should only be used to create qualitative conclusion about anchor behavior. This is assuming that anchor behavior in Laponite gel is comparable soil. By modeling anchor trajectory in the Laponite Tank with an analytical method developed for use with soil this assumption can be examined.

5.2 Analytical Method

The analytical method presented in Aubeny et al. (2009) was selected for creating an analytical model. It is assumed that normalized anchor line tension was constant throughout testing in the Laponite Tank, this is inherent in Eq. (5.1) from Aubeny et al. (2009). Fig. 5.1 presents the anchor system modeled.

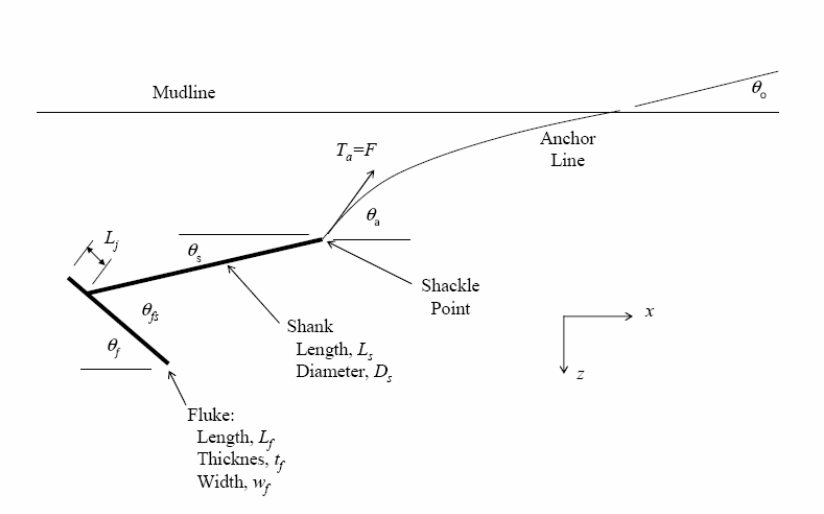

Fig. 5.1: Schematic of anchor system (Aubeny et al., 2009)

$$\frac{d\theta_a}{d\hat{z}} = \frac{\left(\frac{E_n N_{ca}}{\hat{T}_a} - \frac{\theta_a^2 - \theta_0^2}{2(1/\eta + \hat{z})}\right)}{\left(\theta_a - \theta_0 \frac{d\theta_0}{d\theta_a}\right)} \tag{5.1}$$

where: $\hat{z}$ = normalized depth of shackle = z/b

$\hat{T}_a$ = normalized tension at shackle = $T_a/S_{ua}b^2 = N_{eq}A_f/b^2$

b = anchor line diameter

S_{ua} = soil shear strength at the shackle

T_a = Tension at the shackle = $S_{ua}A_f N_e$

θ_a = anchor line angle at the shackle

θ_0 = anchor line angle at the mudline

η = normalized strength gradient parameter = bk/S_{u0}

S_{u0} = soil shear strength at the mudline

N_{ca} = bearing factor for anchor line

E_n = multiplier for anchor line comprised of chain

k = soil shear strength gradient parameter

N_{eq} = dimensionless load factor

z = depth

To utilize the above equation for modeling the Laponite Tank certain considerations must be taken. As noted in Subsection 4.1.3 the shear strength of Laponite gel is not readily measurable. Therefore shear strength S_{u0} and the soil strength gradient

parameter k are unknown. The soil strength gradient parameter will be assumed small. This assumption will essentially simplify Eq. (5.1) to Eq. (5.2). As a result anchor trajectory will no longer be dependent on soil shear strength. Thus, meaningful trajectory predictions can be made without knowing the shear strength of Laponite gel:

$$\frac{d\theta_a}{d\hat{z}} = \frac{(\frac{E_n N_c}{\hat{T}})}{(\theta_a - \theta_0 \frac{d\theta_0}{d\theta_a})} \tag{5.2}$$

The following algorithm describes how to calculate the anchors trajectory from Eq. (5.1) and was developed from similar algorithms found in Aubeny and Chi (2010a) and Aubeny and Kim (2008). This algorithm has been updated for the assumption that rate of change in normalized tension is zero and rate of change of anchor line angle at the mudline $d\theta_0$ does not equal zero.

1. The anchor is displaced an increment Δ_t parallel to the fluke. This displacement is then broken into vertical and horizontal displacements Δ_z and Δ_x respectively.
2. The change in anchor line angle at the shackle $d\theta_a$ is calculated with update normalized depth increment $d\hat{z}$ and normalized depth z.
3. Anchor line angle at the shackle point θ_a and orientation of the fluke are then update by summing with $d\theta_a$.
4. Depth and horizontal displacement are updated by summing the incremental Δ_z and Δ_x values to x ans z, respectively.
5. Soil shear strength S_{ua} is updated for the new depth.
6. Change in anchor line angle at the mudline $d\theta_0$ with respect to the change in

anchor line angle at the shackle point $d\theta_a$ is updated.

7. The anchor line angle at the mudline θ_0 is update from catenary equations.
8. Repeat steps 1-6 until the fluke orientation approaches zero.

By using either Eq. (5.1) or Eq. (5.2) and the preceding algorithm it is possible to analytically model experiments conducted in the Laponite Tank. Making it possible to qualitatively establish the legitimacy of the experiments conducted in the tank.

5.3 Computer Program

The Laponite Tank was modeled with a computer program created by Dr. Charles Aubeny at Texas A&M University that utilizes the algorithm presented above. This program was written in MATLAB. The program *LapTraj* calculates anchor trajectory using Eq. (5.1). Slight editing was required for modeling the Laponite Tank. This was superficial and only impacted user inputs and outputs.

The program *LapTraj* is limited in it's ability to model the Laponite Tank. As noted in the algorithm the anchor line angle at the mudline is allowed to change and impact trajectory. This accomplished by assuming the anchor line behaves as an inverse catenary in the soil, the anchor line is attached to a point at a set height above the mudline, and the anchor line length is finite and constant. In the tank the assumption that anchor lines be have as inverse catenaries is not unreasonable. The anchor line guidance system is configured such that the anchor line pivots about a point at a set height above the mudline (Subsection 4.1.1). However, anchor line length is not constant. As embedment occurs the anchor anchor line length decreases.

The effect of anchor line shortening is minimal while the anchor line angle at the mudline θ_0 is small. As θ_0 increases the anchor line will become taught the anchor begin to plow vertically towards the surface. This effect can be seen in the example provided in Fig. 5.2. This behavior is not well understood. The program *LapTraj* can only effectively model experimentation from the Laponite Tank for small anchor line angles at the mudline.

The program requires 17 inputs these have been listed in Table 5.1. Many of the inputs are self-descriptive; however, the following discussion covers issues unique to the Laponite Tank. These include the soil gradient value, soil shear strength at the mudline, and bearing factors.

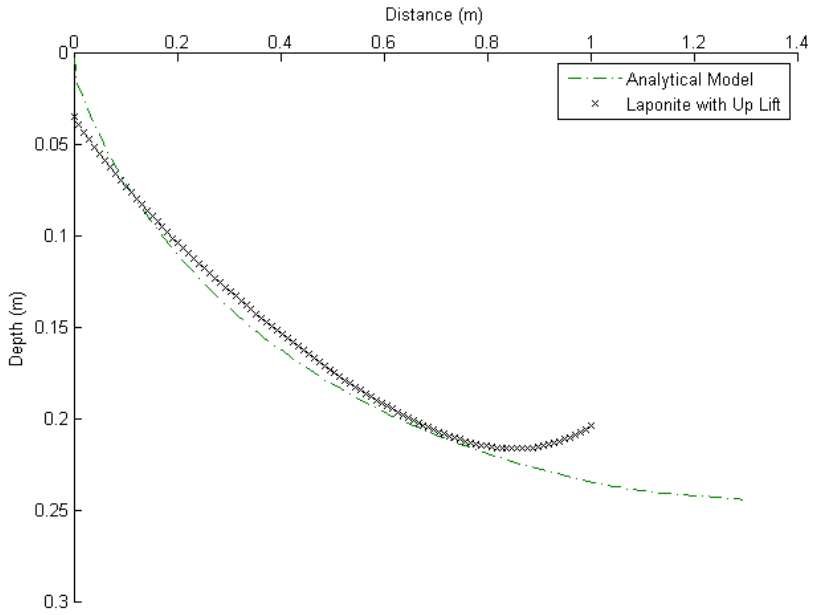

Fig. 5.2: Example of uplift due to line shortening comparative to analytical model

The soil gradient parameter k is assumed small. A parametric study was conducted to establish a value k of which does not impact trajectory. This study can be found in Subsection 5.4.1.

As indicated previously anchor trajectory is not dependent of soil shear strength S_{u0} when the soil gradient parameter is small. The program *LapTraj* requires a value of soil shear strength to prevent division by zero. The value assigned to S_{u0} will not impact

trajectory. For all programs runs S_{u0} is assigned a value of one.

Table 5.1: Inputs for the program *LapTraj*

Program Traits	
Filename	File name for delimited text file output of trajectory
ds	Incremental step size
x_stop	Maximum x displacement
units	Unit selection (SI=1, English=0)
Anchor Properties	
Af	Fluke area
Ne	Load capacity factor
qaf	Initial angle between fluke and anchor line
Anchor Line Properties	
b	Anchor line diameter
Nc	Anchor line bearing factor
En	Line type (wire=1, chain=2.5)
mu	Anchor line tangential-normal force ratio
Soil Strength Profile	
Su0	Soil shear strength at mudline
k	Soil shear strength gradient parameter
Initial Conditions	
z0	Initial anchor embedment
x0	Initial horizontal anchor shackle placement
Anchor Line Guidance System	
xw0	Initial horizontal distance between shackle point and guidance system
zw	Height of guidance system above the mudline
Plhe	Plug heave effect variable

Two bearing factors are required for the program *LapTraj*: the load capacity factor N_e and N_{ca} the anchor line bearing factor. The load capacity factor is dependent of the anchor in use, typical values are provided in Aubeny et al. (2008). The anchor line bearing factor is dependent on material properties of the soil. A parametric study was conducted to evaluate N_{ca} for use in *LapTraj*.

The program *LapTraj* has two outputs. A figure containing a plot of DEA trajectory example provided in Fig. 5.3. A tab delimited text file containing the x-y coordinates of DEA trajectory is also produced. The program has the capabilities to output anchor capacity, however these are currently inactive.

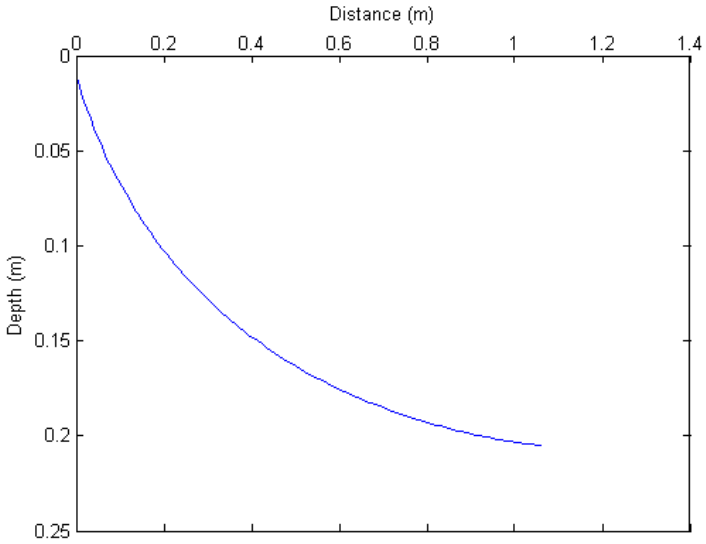

Fig 5.3: Example output plot from *LapTraj*

5.4 Parametric Studies and Results

Three studies were conducted using the program *LapTraj*. This data was used to verify the qualitative capabilities of the Laponite Tank. A parametric study of the soil gradient

parameter was conducted to establish a sufficient value. A parametric study of anchor line bearing factor N_{ca} was conducted to establish a value for Laponite gel. Finally, an examination on the effects of anchor line diameter on anchor trajectory was conducted. This lead to a further investigation of anchor line bearing factor N_{ca} in Laponite gel.

5.4.1 Soil Gradient Parameter

The soil gradient parameter k is the increase in shear strength with depth. For the Laponite tank this parameter is assumed to be small. A sufficiently small soil gradient parameter will have no affect on the DEA trajectory. This value was determined with a parametric study using the program *LapTraj.* DEA trajectories were modeled with soil gradient values of one, 0.1, 0.01 and 0.001 kN/m^3/m.

The program was ran under the following conditions. Fluke area was taken to be 0.0067 m^2. The anchor was assumed to have a fluke-shank angle of 50 degrees. The load bearing factor was taken as 6.7 and anchor line bearing factor was taken as 10, these values were randomly chosen. Geometry was set to that of the Laponite Tank, see Subsection 4. Incremental step size used in the numerical calculations was 0.01 m. The initial angle between the fluke and the anchor line was taken as 50 degrees. These parameters were held constant for all for program runs.

The results from the study can be seen in Fig 5.4. Soil gradient parameters below 0.01 kN/m^3/m appears to have little differential affect on anchor trajectory. A soil gradient parameter k of 0.01 kN/m^3/m or smaller is recommended for modeling the Laponite Tank analytically.

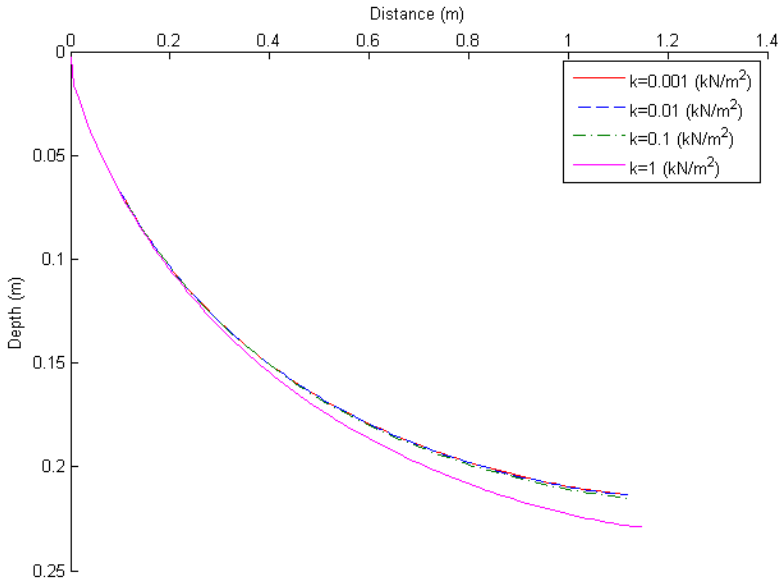

Fig. 5.4: Effect of soil gradient parameter on embedment depth

5.4.2 Anchor Line Bearing Factor

The dimensionless anchor line bearing factor N_{ca} is dependent on the material properties of soil. As the properties of Laponite gel were unattainable this value was determined with a parametric study. Values of N_{ca} were varied over a range of 30 to 50 until the model trajectory matched the experimental data collected from the Laponite Tank.

The following were the condition of the Laponite Tank experiments. The scale anchor used in the tank has an approximate fluke length of 10.16 cm and fluke area of 0.0095 m^2. The anchor shank length was 17.78 cm (seven in). The fluke-shank angle of the anchor was approximately 50 degrees. The anchor has an estimated load bearing factor N_e of five, this value is similar with those from Aubeny et al. (2008). The anchor line diameter was 0.16 cm (1/16 in). Five experimental runs were taken to obtain an average trajectory.

The following parameters were used in the program *LapTraj* for analytically modeling anchor trajectories. Fluke area was 0.0095 m^2. The load bearing factor was set to five. Geometry was set to that of the Laponite Tank, see Section 4. Incremental step size was 0.01 m. The initial angle between the fluke and the anchor line was taken as 50 degrees. These parameters were held constant for all for program runs.

The experimental data used is the same as shown in Subsection 4.3.2, for the parameters given above. The same post processing was conducted. A least squares polynomial regression to the fourth power was preformed on the data set. This best fit line was used for comparison with the analytical model.

Results can be seen in Fig. 5.5. These plots indicate an anchor line bearing factor N_{ca} of 40 is appropriate for an anchor line diameter of 0.16 cm in Laponite gel. Aubeny et al. (2008) indicates and N_{ca} value of 12 being appropriate for soil. The high value found here is probably due to low strength and thixotropic properties of Laponite gel. This result shows that it is possible to model anchor trajectories in the Laponite Tank using current analytical methods. The use as of the Laponite Tank as a qualitative tool is appropriate.

5.4.3 Impact of Anchor Line Diameter on Analytical Model

In Subsection 4.3.2 the effects of change in anchor line diameter were examined with experimentation in the Laponite Tank. A comparison study was conducted with the program *LapTraj*. A strong qualitative correlation would further establish the strength of the Laponite Tank as a qualitative testing apparatus.

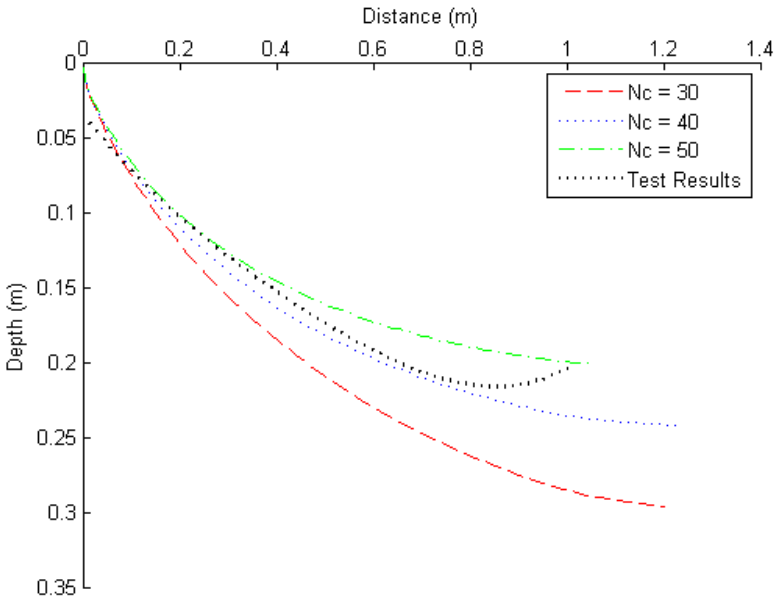

Fig. 5.5: Parametric study of N_{ca} for an anchor line diameter of 1.6 mm

The fourth power polynomial regression of the experimental data used in Subsection 4.3.2 (Fig. 4.30) was plotted in comparison to trajectories obtained from the program *LapTraj*. As in the experimental tests, trajectories were determined for anchor line diameters of 0.96 mm, 1.58 mm (1/16 in) and 3.18 mm (1/8 in). The following were the parameters used in modeling the trajectories. Fluke area was 0.0095 m^2. The load bearing factor was set to five. The anchor line bearing factor was set to 40. Geometry was set to that of the Laponite Tank, see Section 4. Incremental step size was 0.01 m. The initial angle between the fluke and the anchor line was taken as 50 degrees. These parameters were held constant for all for program runs.

The results from this study have been provided in Fig. 5.6. The analytical model indicates a change in anchor line diameter does impact trajectory depth. A larger anchor line diameter will decrease embedment depth and vice-versa. This is consistent with the results found in Subsection 4.3.2 from the Laponite Test. The analytical model however

indicates that a changes in anchor line diameter will have a much larger impact on embedment depth than experimentation in the Laponite Tank shows.

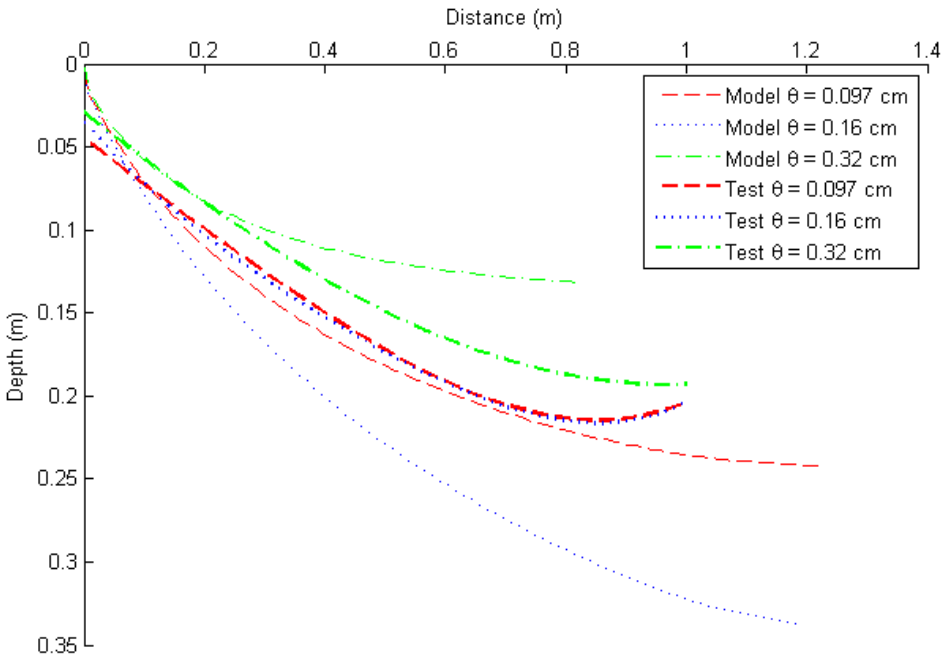

Fig. 5.6: Comparative impact of anchor line diameter on DEA trajectory

Laponite Tank geometry and anchor geometries are constant between tests. Aubeny and Chi (2010a) show the load bearing factor N_e is dependent on anchor geometry and soil shear strength. Both are constant between tests. The resulting conclusion then must be that the anchor line bearing factor N_{ca} must be variable. Aubeny et al. (2008) indicates the anchor line bearing factor N_{ca} remains constant at approximately 12, for a wire in soil. However, it appears that N_{ca} is varying with anchor line diameter in Laponite gel.

Two more parametric studies were conducted to examine the change in the anchor line

bearing factor N_{ca} with anchor line diameter. These were done for anchor line diameters of 0.96 mm and 3.18 mm (1/8 in) and followed the procedure in Subsection 5.4.2. The results for an anchor line diameter of 0.96 mm and 3.18 mm (1/8 in) can be seen in Fig. 5.7 and Fig. 5.8, respectively.

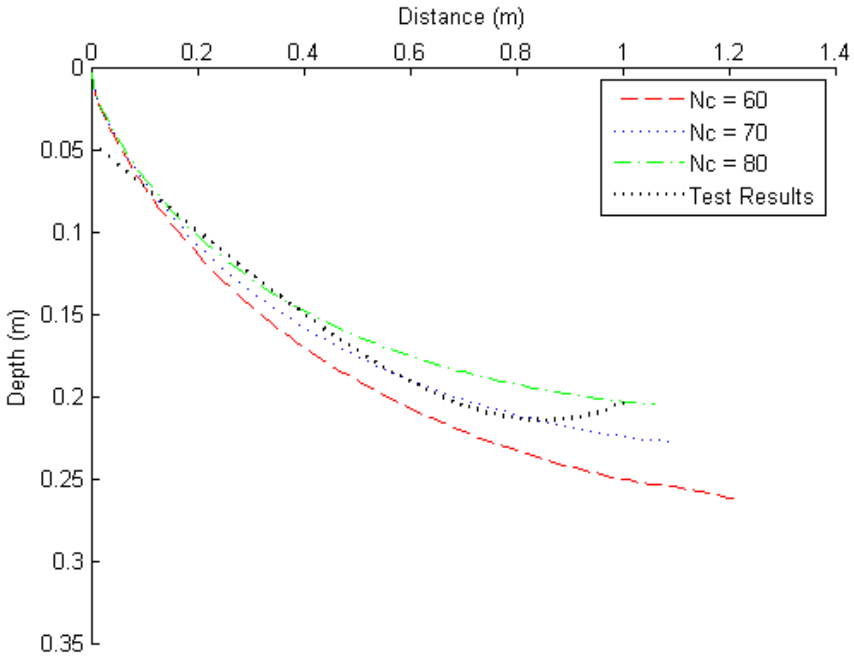

Fig. 5.7: Parametric study of N_{ca} for an anchor line diameter of 0.96 mm

The results show that anchor line diameters of 0.96 mm, 1.6 mm, and 3.18 mm result in an apparent N_{ca} values of 70, 40, and 25 respectively, as seen in Fig. 5.5, Fig. 5.7 and Fig 5.8, respectively. As anchor line diameter increases, the anchor line bearing factor N_{ca} decreases in Laponite gel, Fig. 5.9. This effect is probably due to the thixotropic properties of Laponite gel, noted in Subsection 4.1.3. The material properties of Laponite gel are resulting in smaller anchor line bearing factors for larger anchor line diameters.

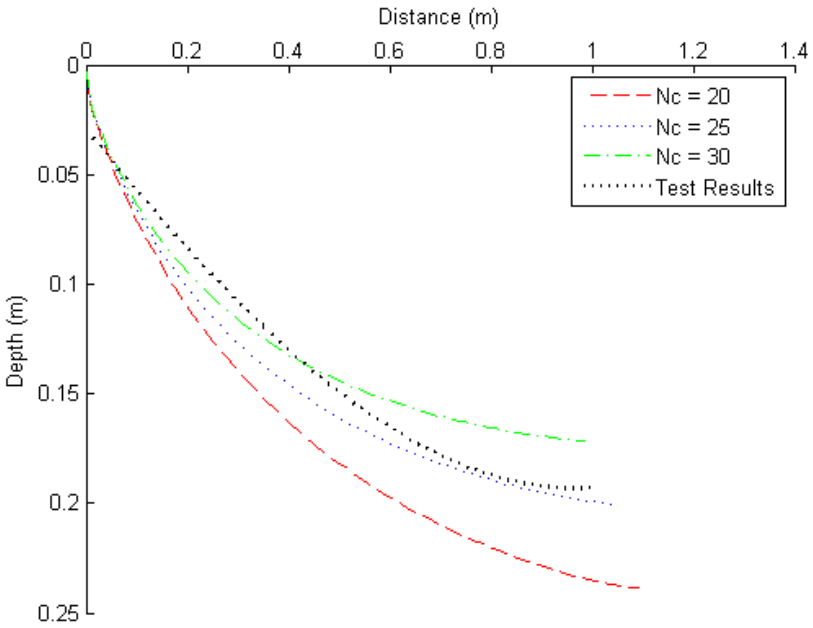

Fig. 5.8: Parametric study of N_{ca} for an anchor line diameter of 3.18 mm

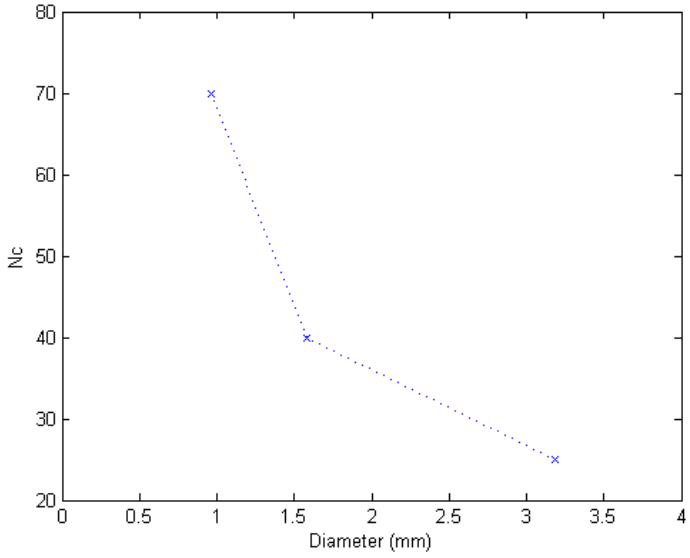

Fig. 5.9: Anchor line bearing factor versus anchor line diameter in Laponite gel

These results show experiments conducted in the Laponite Tank do follow current DEA trajectory methodology. This allows the tank to serve as a reasonable means of making qualitative insights into anchor behavior. However, this anchor line diameter study also shows the thixotropic properties of Laponite gel can cause results which are atypical to soil. As long as these effects are taken into account the Laponite Tank can be an effective qualitative tool.

6 CONCLUSION

6.1 Overview

The research presented in this thesis considered two aspects of anchoring technologies: installation and removal of suction caissons and installation of drag embedment anchors. The use of the Laponite Tank and analytical methods has resulted in new means of modeling and evaluating anchoring technology. These techniques have also opened the door for future research as well. The following is a review of research conducted including concluding remarks and recommendations for future work.

6.2 Analytical Modeling of Suction Caissons

6.2.1 Summary

Two algorithms for calculating required pressures from suction caisson installation and removal were created. These were utilized to develop two computer programs in the MATLAB programming language. These programs are *CaissInGenBeta* and *CaissOutGenBeta*.

The installation program *CaissInGenBeta* was developed using analytical methods presented by Anderson et al. (2005) and programming techniques outlined in Subsection 3.3. The program calculates required and critical under-pressures for a user inputted suction caisson geometry. *CaissInGenBeta* is capable of modeling resistant forces do to internal structural stiffeners. Calibration of soil sensitivity were completed to field data.

The removal program *CaissOutGenBeta* was developed using similar prinicples presented by Anderson et al. (2005), but modified to apply to caisson extraction through application of over pressure. The analytical method in Anderson et al. (2005) is limited to installations. An analytical methods was developed for caisson removal and presented in Subsection 3.2. The program calculates critical and require over-pressures. *CaissOutGenBeta* is capable of modeling resistant force due to internal structural stiffeners. It is also capable of modeling applied external loads placed on the caissons by

a winch during the removal process. Soil sensitivity was calibrated to field data.

6.2.2 Future Work

The development of the analytical method and algorithms for modeling the installation and removal of suction caissons was successful, however it was left room for further development. Specifically, future refinements can include the development of a time dependent suction installation model and for modeling caisson installation in coarse grained soils.

The work presented in Section 3 is essentially independent of time. However, soil properties are time dependent. For an ideal installation, time dependency should be minimal. A time dependent model would be useful for modeling installations or removal where conditions were not ideal; for example, when partial caisson installation is completed after partial consolidation.

The computers programs developed in this research are for fine grained soils. However, the algorithms used in these programs could be adapted for modeling caissons in coarse grain soil.

6.3 Experimental Modeling of Drag Embedment Anchors

6.3.1 Summary

The Laponite Tank was developed as a means of testing the embedment of drag embedment anchors. Laponite gel is a translucent thixotropic colloid. Laponite gel's strength do not exactly mimic soil, making it difficult to make quantitative predictions using the Laponite Tank. However, Laponite gel is transparent allowing the anchors trajectory to be visible and therefore measurable, which is clearly not possible in soil. Scale model testing in the Laponite Tanks provides a means of quick and repeatable testing of DEAs, which field testing cannot economically provided.

Experiments in the Laponite Tank are visually recorded using a video camera. Computer software is then capable of providing the real world Cartesian coordinates of the anchor from the video footage and reference frame size. These coordinates can then be used to

evaluate anchor performance.

Three studies were conducted in the Laponite Tank. First, it was established the the threshold variable will have little impact on measured anchor trajectory. Secondly, it was shown the increasing anchor line diameter will result in shallower embedment depth. Third, it was shown that embeding an anchor with an out of plane load will decrease anchor embedment depths.

6.3.2 Future Work

The Laponite Tank is a successful small scale testing apparatus. It however, does have room for improvement. The addition of new equipment could remove variability and a better video camera would reduce error.

Attaching an electric motor to the Laponite Tank would be useful. Currently anchor embedment is done by manually applying an anchor line force, resulting in a variable embedment rate and an unknown anchor line force. With an electric motor embedment rate could be controlled and anchor line force would be measurable. This would reduce variability and provided more data for analysis.

Currently a standard low resolution consumer camcorder is used for recording tests in the Laponite Tank. If a high definition camera with high grayscale contrast was used, measurement error in anchor trajectory could be reduced. Essentially the higher the contrast between the anchor and the gel the better the results.

6.4 Analytical Modeling of Drag Embedment Anchors

6.4.1 Summary

A computer developed by Dr. Charles Aubeny at Texas A&M University was edited and utilized for evaluating the performance of the Laponite Tank relative to current DEA trajectory analytical methods. Studies were done on the effects of the soil gradient parameter, the anchor line bearing factor, and anchor line diameter.

The program utilizes the analytical methods outline in Aubeny et al. (2009) and Aubeny

and Chi (2010a). The program is capable of modeling anchor trajectories in testing basins. It was edited for Laponite Tank geometry and Laponite gel properties.

A parametric study on the effects of the soil gradient parameter was conducted. The shear strength of Laponite gel is unknown as is the soil gradient parameter. For modeling purposes the soil gradient parameter was assumed zero. However, a soil gradient parameter is required for the program *LapTraj* to prevent division by zero. Various low values of the soil gradient were tested to determined a maximum value which would not affect anchor trajectory.

A study was conducted to determine the anchor line bearing factor N_{ca} for Laponite gel. The value of N_{ca} was varied until the theoretical trajectory was fitted to the experimental results. Traditionally this value is only impacted by soil properties for a wire anchorline.

Finally, a study of the anchor line diameter on anchor trajectory completed. This was done for comparison of results obtained in the Laponite Tank in Section 4. The results were found fit the general trend but magnitudes were significantly different. Further examination yielded a correlation between anchor line diameter and anchor line bearing factor. For drag embedment in soils the anchor line bearing factor for typical anchor lines is essentially independent of anchor line diameter. However, the thixotropic properties of Laponite gel appear to make them dependent on anchor line diameter for the case of Laponite gel. Anchor line bearing factors as a function of anchor line diameter were determined and plotted.

6.4.2 Future Work

Analytical modeling of the Laponite Tank proved useful; however, raised many questions. Especially surrounding Laponite material properties and model anchor line behavior. Future research in these areas would be helpful.

Laponite material properties are proving to be quite different from that of soil. With combined use of the Laponite Tank and the program *LapTraj* a better understanding

could be obtained. Specifically, further examination of bearing factors in Laponite would be useful.

Analytical methods and modeling algorithms also currently lack a means modeling an anchor line which decreases in length during installation. Though this is traditionally an atypical scenario it is how embedment occurs in the Laponite Tank. Anchor trajectory behavior for small angles at the mudline can be modeled successfully with current techniques. However, the behavior of full embedment cannot be examined with the Laponite without further knowledge of anchor line shortening effects.

REFERENCES

Anderson, K. H., Murff, J. D., Randolph, M. F., Cluckey, E. C., Erbrich, C. F., et al. 2005. "Suction anchors for deepwater application." *Proc., Int. Symp. on Frontiers in Offshore Geotechnics, IS-FOG05*, Balkema, Perth, Australia, 3–30.

Aubeny, C. P., Beemer, R. D., Zimmerman, E. (2009). "Soil impact on non-stationary Anchor Preformance." *Proc., Offshore Technology Conf. 2009*, OTC 20081, Houston.

Aubeny, C. P., and Chi, C. (2010a). "Mechanics of drag embedment anchor in a soft seabed," *J. of Geotech. and Geoenvir. Engrg.*, 136(1), 57-68.

Aubeny, C.P., and Chi, C., (2010b). "Trajectory prediction for drag embedment anchors under out of plane loading." *Proc., Int. Symp. on Frontiers in Offshore Geotechnics, IS-FOG10*, Balkema, Perth, Australia, 699-703.

Aubeny, C. P., Kim, B. M., and Murff, J. D. (2008). "Prediction of anchor trajectory during drag embedment in soft clay." *Int. J. Offshore Polar Eng.*, 184, 314–319.

Aubeny, C. P., Murff, D. J., and Roesset, J. M. (2001). "Geotechnical issues in deep and ultra deep waters." *Int. J. Geomech.*, 1(2), 225–247.

Chi, C. (2010). "Plastic limit analysis of offshore foundation and anchor." PhD Dissertation, Texas A&M Univ., College Station, TX.

Han, S. (2002). "The capacity of suction caisson in isotropic and anisotropic cohesive soils under general loading condition." PhD Dissertation, Texas A&M Univ., College Station, TX.

Kim, B. M. (2005). "Upper bound analysis for drag anchors in soft clay." PhD Dissertation, Texas A&M Univ., College Station, TX.

McAndrew, A., (2004). *Introduction to digital image processing with MATLAB.,* Thomson/Course Technology, Boston, MA.

Moon S., (2000). "Lateral resistance of suction caisson anchors." ME Project, Texas A&M Univ, College Station, TX.

Sharma, P. P., (2004). "Ultimate capacity of suction caisson in normally and lightly overconsolidated clays." MS thesis, Texas A&M Univ, College Station, TX.

Veniamin A., (2006). “Comparison of Degenkamp and Randolph solutions to predict embedded mooring chain profile and anchor-chain tension.” ME Project, Texas A&M Univ, College Station, TX.

Yang, M. (2008). “Undrained behavior of plate anchors subjected to general loading.” PhD Dissertation, Texas A&M Univ., College Station, TX.

Yoon, Y. (2002). “Prediction methods for capacity of drag anchors in clayey soils.” MS thesis, Texas A&M Univ, College Station, TX.

VITA

Name:	Ryan Deke Beemer
Address:	Texas A&M University Zachary Department of Civil Engineering 3136 TAMU College Station, TX 77843-3136
Email Address:	rdbeemer@tamu.edu
Education:	B.S., Civil Engineering, Minor, Mathematics, Washington State University, 2004 M.S., Civil Engineering, Texas A&M University, 2011